The FEBS Journal

FEBS PRESS science publishing by scientists

Functional characterization of Fur from the strict anaerobe *Clostridioides difficile* provides insight into its redox-driven regulatory capacity

Ángela Fernández-Otal[1,2,3], Jorge Guío[1,2], Cristina Sarasa-Buisan[1,2], M. Luisa Peleato[1,2], María F. Fillat[1,2], Ángel Lanas[3,4,5] and M. Teresa Bes[1,2]

1 Department of Biochemistry & Molecular and Cellular Biology, University of Zaragoza, Spain
2 Institute for Biocomputation and Physics of Complex Systems (BIFI), Mariano Esquillor (Edif. I+D), Zaragoza, Spain
3 Aragon Institute for Health Research (IIS Aragón), Zaragoza, Spain
4 Digestive Diseases Service, University Clinic Hospital Lozano Blesa, Zaragoza, Spain
5 CIBERehd, Madrid, Spain

Keywords
Clostridioides difficile; ferric uptake regulator; iron metabolism; oligomerization; oxidative stress; thioredoxin

Correspondence
M. T. Bes, Department of Biochemistry & Molecular and Cellular Biology, University of Zaragoza. Pedro Cerbuna 12, 50009 Zaragoza, Spain
Tel: (+34) 976 762479
E-mail: tbes@unizar.es

Ángela Fernández-Otal and Jorge Guío contributed equally to this article.

(Received 1 December 2023, revised 6 February 2024, accepted 29 April 2024)

doi:10.1111/febs.17156

Clostridioides (formerly *Clostridium*) *difficile* is a leading cause of infectious diarrhea associated with antibiotic therapy. The ability of this anaerobic pathogen to acquire enough iron to proliferate under iron limitation conditions imposed by the host largely determines its pathogenicity. However, since high intracellular iron catalyzes formation of deleterious reactive hydroxyl radicals, iron uptake is tightly regulated at the transcriptional level by the ferric uptake regulator Fur. Several studies relate lacking a functional *fur* gene in *C. difficile* cells to higher oxidative stress sensitivity, colonization defect and less toxigenicity, although Fur does not appear to directly regulate either oxidative stress response genes or pathogenesis genes. In this work, we report the functional characterization of *C. difficile* Fur and describe an additional oxidation sensing Fur-mediated mechanism independent of iron, which affects Fur DNA-binding. Using electrophoretic mobility shift assays, we show that Fur binding to the promoters of *fur*, *feoA* and *fldX* genes, identified as iron and Fur-regulated genes *in vivo*, is specific and does not require co-regulator metal under reducing conditions. Fur treatment with H_2O_2 produces dose-dependent soluble high molecular weight species unable to bind to target promoters. Moreover, Fur oligomers are dithiotreitol sensitive, highlighting the importance of some interchain disulfide bond(s) for Fur oligomerization, and hence for activity. Additionally, the physiological electron transport chain NADPH-thioredoxin reductase/thioredoxin from *Escherichia coli* reduces inactive oligomerized *C. difficile* Fur that recovers activity. In conjunction with available transcriptomic data, these results suggest a previously underappreciated complexity in the control of some members of the Fur regulon that is based on Fur redox properties and might be fundamental for the adaptive response of *C. difficile* during infection.

Abbreviations
CD, circular dichroism; DTNB, 5,5′-Dithiobis-(2-nitrobenzoic acid); DTT, dithiothreitol; EMSA, electrophoretic mobility shift assay; Fur, Ferric Uptake Regulator; HMW, high molecular weight; ICP-OES, Inductively Coupled Plasma Optical Emission spectroscopy; IPTG, isopropyl ß-D-1-thiogalactopyranoside; NTA, nitrilotriacetic acid; NTR, NADPH-dependent thioredoxin reductase; PAR, 4-(2′-Pyridylazo)-resorcinol; PMSF, phenylmethylsulfonyl fluoride.

The FEBS Journal **291** (2024) 3604–3627 © 2024 The Authors. *The FEBS Journal* published by John Wiley & Sons Ltd on behalf of Federation of European Biochemical Societies.

Introduction

Clostridioides difficile, formerly *Clostridium difficile* [1], is a gram-positive, spore forming anaerobic bacterium recognized as the etiological agent of almost 30% of antibiotic associated diarrhea and as the major cause of colitis in developed countries [2]. This pathogen has gained notoriety due to the emergence of hypervirulent strains, sometimes refractory to standard therapies, which have dramatically changed the epidemiology and severity of *C. difficile* infections in Europe and North America [3,4]. Although many processes can influence resistance to antibiotics of this pathogen, an increasing number of studies relate resistance to some drugs with altering both the expression of redox proteins and iron metabolism [5]. A shotgun proteomics approach used to compare differences in the proteomes of *C. difficile* isolates treated with metronidazole, a first-line therapy against this pathogen, suggested that iron uptake could be diminished after treatment with metronidazole in a resistant strain [6]. In the same way, analysis of a metronidazole-resistant RT010 *C. difficile* strain using a quantitative proteomic approach suggested deficient iron storage on mid-log-phase cultures [7]. In addition, colonization process by *C. difficile* appears to be facilitated by several genes involved in iron uptake or in response to oxidative stress, according to the analyses of the genome-wide temporal expression of *C. difficile* genes during the first 38 h of mouse colonization [8] or the behavior of a *feoB1* deletion mutant in *C. difficile* R20291 [9]. In this sense, the importance of iron as a nutrient for *C. difficile* is evidenced by the transcriptional changes undergone by this microorganism when grown in an iron-limited environment. Specifically, iron acquisition and iron stress adaptation systems, among others, are induced [10].

Control of iron homeostasis in most pathogenic bacteria is mediated by the ferric uptake regulator (Fur), which regulates the expression of genes involved in iron uptake and storage in response to iron availability [11]. Fur is a transcriptional regulator identified in numerous bacteria functioning primarily as a repressor of the transcription of iron uptake-related genes [12]. However, Fur also regulates transcription of a plethora of genes involved in other physiological processes including defenses against oxidative stress, virulence factors, DNA replication, cell morphology or redox regulation, among others [13–18]. In its classical model of regulation, Fur functions as a holo-repressor of gene transcription. Upon binding of ferrous iron under this nutrient sufficient conditions, the complexes Fur-Fe^{2+} associate as dimers to *cis* regulatory elements known as "iron boxes," located in the promoter regions of target genes [19]. Affinity of Fur for iron enables the bacterium to acquire the amount of metal necessary to build essential iron-containing and utilizing proteins. Nevertheless, when iron quantity overtakes that needed for these proteins function, Fur represses transcription of iron uptake mechanisms to avoid overload of this metal and thereby preventing iron toxicity associate to Fenton reactions [20]. In addition, other regulatory mechanisms have been described, indicating that Fur can also bind to specific target promoters in its apo form [21]. Moreover, apo- and holo-Fur activation have also been documented [11].

Protein folding exhibited by members of the Fur family of transcriptional regulators consists of two functional domains: an N-terminal DNA-binding domain and a C-terminal dimerization domain, harboring a regulatory metal binding site. Located at the beginning of the dimerization domain, the amino acid sequence of many Fur homologs includes a histidine-rich motif HHXHXXCXXC that contains a CXXC motif. Moreover, a less conserved CXXC motif can also be found close to the C-terminus [22]. Crystal structures of several Fur homologs have demonstrated the existence of two or three metal atoms coordinated by amino acid residues of these motifs. Although the regulatory metal binding site shows some variability in metal coordination depending on the Fur homolog, it seems to be quite conserved and involves amino acids from both domains of the regulator [22,23]. Cysteine residues of both CXXC motifs can be implicated in either the coordination of the so-called structural zinc atom, found in Fur structures from *Helicobacter pylori* [24] and *Campylobacter jejuni* [25], or can shape a thiol/disulfide redox switch that determines Fur ability to bind the metal corepressor, as described in cyanobacterial FurA [26].

Microarray analysis comparing transcriptional differences between a *C. difficile fur* mutant and the wild-type strain demonstrated that *C. difficile*, like other pathogenic bacteria, regulates expression of several putative iron acquisition systems using the transcriptional regulator Fur. Iron uptake mechanisms appeared induced both under iron limiting conditions *in vitro* and during *C. difficile* infection of the host [27]. According to these studies, Fur seems to function as a global transcriptional regulator in *C. difficile*, affecting the expression of more than 70 transcriptional units belonging to different functional categories [27]. In the same way, later results combining

RNA-sequencing-based transcriptomic, metabolomic and electron microscopy approaches to characterize multiple functional and metabolic changes induced by the Fur-mediated low iron response confirmed that other functions besides iron regulation are executed by Fur in *C. difficile* [28]. Additionally, Fur from *C. difficile* (hereafter *Cd*Fur) seems to play a role in the adaptive strategies used by this anaerobic bacterium to respond to low oxygen concentration exposure [29]. In fact, *C. difficile fur* mutant is more sensitive to H_2O_2, suggesting a role of Fur in the oxidative stress response. Indeed, *Cd*Fur affects transcription of the gene encoding the antioxidant thioredoxin 2 (*trxA2*) and, although it does not directly regulate thioredoxin reductase transcription (*trxB3*), it alters the protein level in the cell [28]. Finally, single nucleotide polymorphism variation in the *fur* gene has been associated to metronidazole resistance in *C. difficile* [30].

Despite the apparent relevance of iron and Fur in the strategies employed by *C. difficile* to ensure optimal viability and virulence, little is known about the biochemical characteristics of *Cd*Fur and its mechanism of action [27,31]. Previous attempts to recombinantly express and purify biologically active *Cd*Fur from *Escherichia coli* failed, since protein preparations appeared inactive [27]. Herein, we have successfully obtained recombinant active *Cd*Fur to address a biochemical and functional characterization of this regulator that, as far as we know, provide the first clues of the molecular mechanism that modulates the regulatory function of Fur in a strict anaerobic pathogen. First, we show that the recombinant protein is active, developing iron-dependent repression of a Fur-regulated promoter in *E. coli*. Then, using electrophoretic mobility shift assays (EMSAs) we prove that *Cd*Fur can interact specifically with the promoters of its regulon genes *fur*, *feoA*, and *fldX* in the absence of corepressor metal, although these genes are iron- and Fur-regulated *in vivo*. In addition, we show that *Cd*Fur displays a thiol-based oxidation responsive DNA-binding activity on these promoters. We also demonstrate that, in the presence of H_2O_2, *Cd*Fur oligomerizes in a dose-dependent manner, and that this oligomerization can be reverted by thioredoxin. Besides, we provide experimental evidence that demonstrates the DNA-binding activity of a Fur homolog after reduction by thioredoxin. Finally, by correlating of our results with the information about the *Cd*Fur *in vivo* function gained from available transcriptomic data, we discuss the possibility that *Cd*Fur might respond to potential oxidative stress under iron limitation by implementing redox regulation independent of iron.

Results

*Cd*Fur functionally complements a *fur* deletion mutant of *E. coli*

The genome sequence of the *C. difficile* reference strain ATCC 43255 used in this study to clone the Fur protein encodes a predicted Fur homolog in locus UAB_RS0207325. This gene shows 100% amino acid sequence identity to CD630_12870 of reference strain *C. difficile* 630, previously identified by Ho and Ellermeier [27] as the gene encoding the *C. difficile* Fur protein. Ho and Ellermeier cloned and overexpressed *C. difficile* Fur protein in *E. coli* but the purified recombinant protein was inactive [27]. In order to determine whether the *C. difficile fur* gene cloned in the present study encoded a functional Fur protein, we tested the ability of the recombinant *Cd*Fur to functionally complement an *E. coli* Fur-deficient strain. Plasmid pACYC-*furCd* carrying a complete copy of the *fur* gene from *C. difficile* ATCC 43255 was transformed into the *E. coli fur*-deficient strain H1780. This *E. coli fur* mutant carries a chromosomally embedded *fiu-lacZ* fusion that serves as reporter of heterologous Fur activity [32]. The strain expresses *fiu-lacZ* constitutively, in a manner unaffected by iron, so that the synthesis of ß-galactosidase is markedly inhibited when a functional Fur and the corepressor Fe^{2+} are present. For the phenotypic analyses, transformed H1780 *E. coli* cells were grown in MacConkey plates [33]. This selective medium allows distinguishing cells with ß-galactosidase activity (Lac^+ phenotype) by the red color they develop. Plates were supplemented with either 100 μM $FeCl_3$ or 200 μM 2,2′-dipyridyl iron chelator, to determine ß-galactosidase activity in presence or absence of Fe^{2+}, respectively. On iron-deficient MacConkey agar plates (Fig. 1A), transformed cells appeared as red colonies, indicating expression of ß-galactosidase. On the contrary, iron-rich conditions led to colonies with a fainter color (Fig. 1B), indicating a decrease in the synthesis of ß-galactosidase. The observed colors suggested that recombinant *Cd*Fur was a functional Fur homolog capable of developing iron-dependent repression *in vivo*.

*Cd*Fur forms intra- and intermolecular disulfide bonds

The *C. difficile fur* gene encodes a putative 152 amino acid polypeptide with a theoretical molecular mass of 17 586 Da, according to the ProtParam tool available in the EXPASY Server (https://web.expasy.org/protparam/). Its primary structure contains the

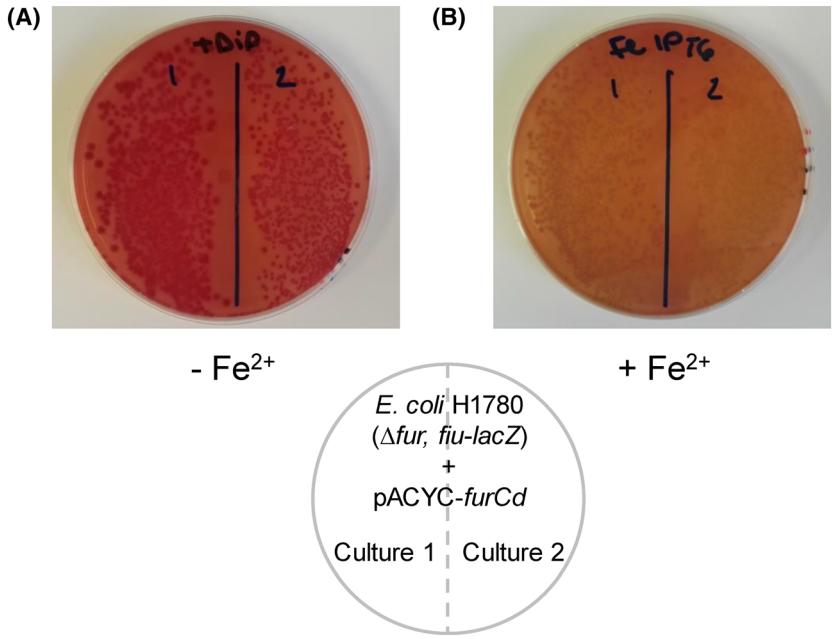

Fig. 1. Evidence that recombinant *Cd*Fur is functional *in vivo*. Expression of the *Cdfur* gene represses the transcription of the *E. coli fiu* gene in an iron-dependent manner. To visualize *fiu-lacZ* expression, MacConkey agar plates were used and two independent *E. coli* strain H1780 cultures carrying pACYC-*furCd* plasmid (Cultures 1 and 2 as indicated in the black and white circular template) were tested. Plates were supplemented with 200 mM 2,2′-dipyridyl (A) or with 100 mM $FeCl_3$ (B) and maintained at 37 °C for 16–18 h. Red indicates strong ß-galactosidase activity, whereas yellow denotes no/low ß-galactosidase activity. The shown images are representative of two experiments.

H_{94}NHHHLICKNC$_{104}$ sequence (Fig. 2), which is analogous to the potential metal binding motif HHXHXXCXXC that has proven to be useful in the purification of Fur homologs and their mutants using metal affinity chromatography (Fig. 2) [34–36]. Therefore, we tried previous purification schemes based on different metal-iminodiacetate chromatographies (Ni, Zn, Cu, and Co) of the histidine-rich motif, but the purification recoveries of recombinant *Cd*Fur were low and insufficient to address a thorough biochemical characterization. Consequently, we optimized a purification protocol based on a His-tagged fusion protein from pET28a(+) plasmid. We chose nickel for the affinity chromatography since the use of zinc and other metals resulted in lower yields. The majority of *Cd*Fur typically eluted from the Ni-NTA column in early fractions and the method yielded around 15 mg of His-tagged purified protein per liter of bacterial culture. Analysis of purified *Cd*Fur by MALDI-TOF after removing the His-tag resulted in a molecular weight value of 17 853 ± 0.2 Da. It included two additional residues (arginine and glycine) that remained in the polypeptide chain after digestion with thrombin of the His-tag. Far UV CD analysis of recombinant *Cd*Fur showed spectral characteristics typical of a α-helix rich protein with minima around 209 and 222 nm (Fig. 3A). This result was in good accordance with the predicted secondary structure calculated using the PSIPRED server protein secondary structure prediction algorithm (http://bioinf.cs.ucl.ac.uk/psipred/) [37], that envisioned four α-helixes in *Cd*Fur N-terminal domain while the C-terminal domain consisting of both α-helixes and ß-sheets (Fig. 3B). The secondary structure motif distribution obtained was analogous to that shown by other Fur homologs whose 3D-structure had already been solved [24,38,39].

When purified *Cd*Fur underwent SDS/PAGE under non-reducing conditions (no DTT or ß-mercaptoethanol in the sample buffer) most of the protein migrated to the monomer position [90% according to quantification with the Multi-Analyst program on GelDoc 2000 images (Bio-Rad Laboratories, Milan, Italy)], (Fig. 4A, lane 1). Reducing conditions (treatment of purified protein with 10 mM of DTT for 10 min) revealed that the monomer band corresponded to a doublet. Specifically, under reducing conditions, the slower migrating component band of the doublet decreased its intensity whereas the faster migrating band seemed to get thicker (Fig. 4A, lane 2). Apparently, both bands corresponded to two Fur isoforms, with the slower migrating band containing

```
                                                                  HHXHXXCXXC
CdFur           -MANTMDLLKDKLKETGFKITPQRRAIVEILLKHDHS-HLSSEEIYDLVRVDCPEIGLAT
Anabaena FurA   MTVYTNTSLKAELNERGWRLTPQRETILHIFQELPQGEHLSAEDLYHRLEADGEGISLST
                  . *   ** :*:* *:::****.:*:.*: :  :. ***:*::*. :..*   *.*:*

                                                                  HHXHXXCXXC
CdFur           VYRTMQLLDEIGLISKLNLDDGCIRYEISLHKEDCHNHHHLICKNCGKIMEAKEDLLDNI
Anabaena FurA   IYRTLKLMARMGILRELELGEGHKHYEINQPYP--HHHHHLICVKCNSTIEFKNDSILKI
                :***::*: .:*:: :*:*.:*  :***.      *:****** :*.. :* *:* : :*

                                    CXXC
CdFur           EKEIQSLYKFKILDHDVKFYGLCDECNGVSDSEE
Anabaena FurA   GAKTAQKEGFHLLDCQMTIHAVCPKCQRALMPL-
                  :  .   *::** ::.:::.:* :*: .  .
```

Fig. 2. Sequence alignment of *C. difficile* Fur (CD630_12870) and *Anabaena* sp. PCC 7120 FurA (All1691) proteins. Pairwise sequence alignment was performed with UniProt ClustalO (https://www.expasy.org/resources/uniprot-clustalo). The corresponding UniProt IDs of *C. difficile* Fur and *Anabaena* sp. PCC 7120 FurA are Q18BE9 and Q7A2F4 and were obtained from (https://www.uniprot.org). The metal binding motif, rich in histidine residues (marked in bold and blue) and useful for purification of the Fur homolog from *Anabaena* sp. PCC 7120 and its mutants, is highlighted in yellow. *C. difficile* Fur cysteines are marked in red and bold. *C. difficile* Fur cysteines that align to redox responding CXXC motifs in Fur from *Anabaena* sp. PCC 7120 (also marked in red and bold) are highlighted in green. The CXXC motifs are indicated with a black box.

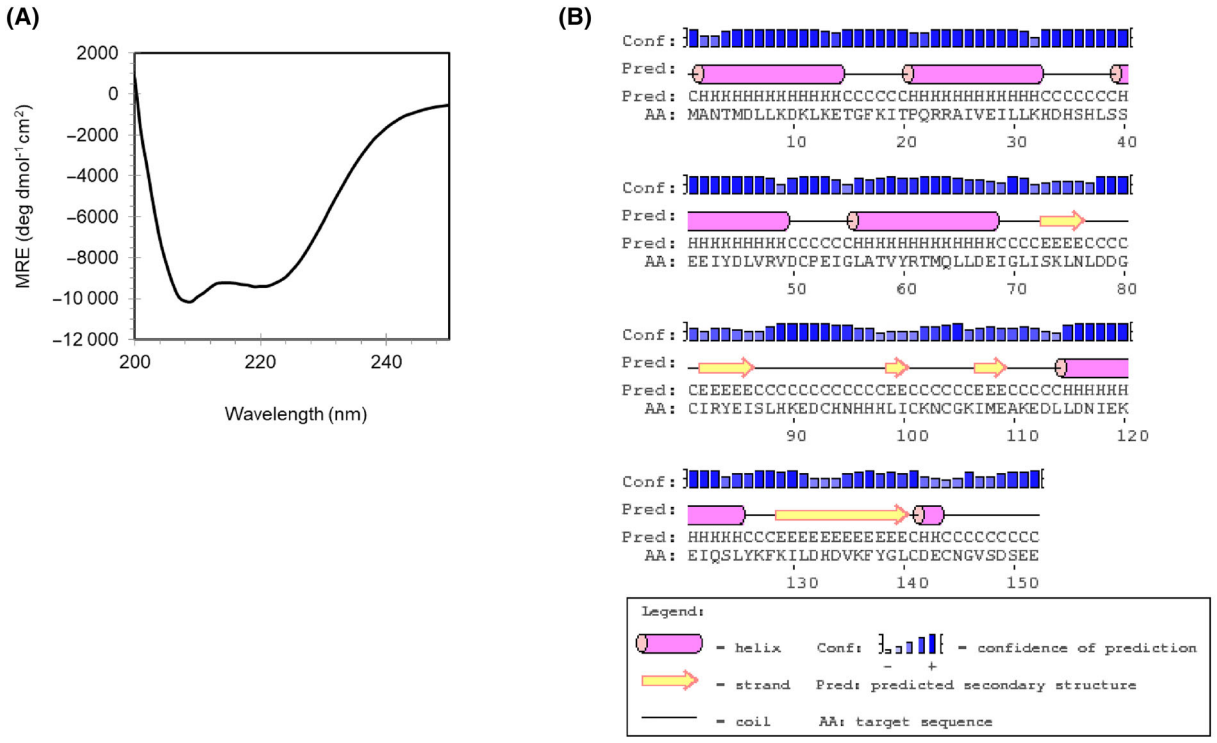

Fig. 3. Secondary structure analyses of *Cd*Fur. (A) Far-UV CD spectrum of *Cd*Fur. The CD measurement was carried out in a Chirascan spectropolarimeter using 0.1 cm cuvettes at 25 °C. Spectrum was recorded with 20 μM protein solution in 50 mM Tris/HCl pH 8. Measurements were performed twice with each replicate scanned five times. CD, circular dichroism; *Cd*, *C. difficile*; Fur, ferric uptake regulator. (B) Secondary structure prediction for Fur from *C. difficile*. Data were obtained using the PSIPRED web server (http://bioinf.cs.ucl.ac.uk/psipred/). According to the web server information, "Conf" indicates confidence of the prediction and is greater the higher the bar is, "Pred" shows the predicted secondary structure elements [cylinder, α-helix (the corresponding amino acids are labeled with H); arrow, β-sheet (the corresponding amino acids are labeled with E); line, absence of regular secondary structure (the corresponding amino acids are labeled with C)], finally "AA" denotes the amino acids of the protein sequence used as the target for the prediction of protein secondary structure.

some intramolecular disulfide bond whose reduction converted that isoform in the fast migrating band. Moreover, the band that migrated to the dimer position in the gel disappeared, which suggested that its formation was mediated by disulfide bonds (Fig. 4A, lanes 1 and 2).

Further treatment of the purified *Cd*Fur protein with increasing concentrations of H_2O_2 led to a gradual loss of the monomer and substantial increase of high molecular weight (HMW) oligomers of *Cd*Fur (Fig. 4B, lanes 1–6). As *Cd*Fur sequence contains seven cysteine residues with possible differences in sensitivity to oxidation, we used supraphysiological peroxide concentrations (250 μM to 10 mM) chosen to gradually oxidize cysteines with high sensitivity to oxidation (oxidized at lower peroxide concentration) and observe high-stoichiometry oxidation of some cysteines with moderate to low sensitivity to oxidation [40]. It is noteworthy, that at 10 mM (highest concentration of peroxide used) there was still monomer left, suggesting that the oxidation capacity of the system was not completely overwhelmed (Fig. 4B, lane 6). Importantly, the formation of HMW oligomers was totally reversed by DTT and a concomitant thickening of the monomer band was observed (Fig. 4B, lane 8), thus suggesting that the H_2O_2-induced formation of HMW species was reversible and that *Cd*Fur oxidation was mediated by intermolecular disulfide bonds.

Recombinant *Cd*Fur protein contains zinc

As *Cd*Fur has seven cysteine residues in its amino acid sequence, four of them arranged in two separated CXXC motifs (Fig. 2), the possibility arose that *Cd*Fur bound some zinc atom [24,25]. Analysis of metal content of the purified recombinant *Cd*Fur using inductively coupled plasma optical emission spectroscopy (ICP-OES) revealed that 0.73 ± 0.06 mole of Zn^{2+} were present per mole of protein. Errors are expressed as standard deviation calculated from metal determination in two experiments in which each sample was measured in triplicate. *Cd*Fur dialysed overnight against 10 mM EDTA also contained zinc. Total zinc determination performed by ICP-OES on a *Cd*Fur preparation obtained after removing the His-tag rendered 0.69 ± 0.02 mole of Zn^{2+} per mole of protein, suggesting that abundance of His residues present in the His-tag did not significantly contribute to the zinc content of the recombinant *Cd*Fur.

To investigate whether the intramolecular disulfide bond described for the monomer in the previous section affected the presence of zinc in the purified protein, we performed an on-gel Zn^{2+} detection with the PAR reagent, a metallochromic indicator used to monitor the existence of transition metals in purified proteins [41]. As observed in Fig. 4C (lane 1), the two bands of the doublet were colored, suggesting that both oxidized and reduced forms of the monomer may contain zinc, that remained associated to the protein during the electrophoresis in the presence of SDS. Interestingly, the small population of dimer deduced by non-denaturing SDS/PAGE was not colored after PAR detection (Fig. 4C, lane 1), suggesting that it may not contain zinc. This result would support the notion that monomer metalation could be a factor to avoid the formation of species that migrated to dimer position since, apparently, they did not contain zinc [42].

In proteins, zinc can be coordinated by both the sulfur atom of cysteine and nitrogen atom of histidine or by carboxylate anions of aspartate and glutamate [43]. We quantified the accessibility of thiol side chains of wild-type protein as measured by their chemical modification using 5,5′-dithiobis-2-nitrobenzoic acid (DTNB). Approximately two cysteine residues (2.26 ± 0.09) were reactive to DTNB in wild-type *Cd*Fur under non-denaturing conditions. After *Cd*Fur unfolding with 6 M guanidinium chloride (GdmCl), the apparent thiol content increased to approximately four cysteine residues per monomer (4.35 ± 0.11). This behavior suggested that in the native form of the protein two cysteines were completely buried or involved in some interaction that disappeared in the presence of denaturing agent, allowing them to react with DTNB. *Cd*Fur contains an odd number of cysteine residues in its amino acid sequence (seven) and as previously described, the purified protein seems to be mainly a monomer with two types of momeric forms that differ in some disulfide bridges (Fig. 4A, lanes 1 and 2). Therefore, it would be expected that the four free cysteines that react with DTNB were consequence of a different number of disulfide bridges present in both denatured monomeric species. One of them would have five free cysteines (one disulfide bridge) and the other one only three (two disulfide bridges), which would render an average of four free cysteines per monomer in the tested protein solution. These results, although not conclusive, would suggest that the four cysteine residues of both CXXC motifs present in *Cd*Fur amino acid sequence (Fig. 2) would not be simultaneously involved in zinc binding, since both types of monomers seem to contain zinc, as detected by PAR staining (Fig. 4C, lane1), but one of them would have at most three of the cysteines in the thiol form. Apparently, cysteines in *Cd*Fur would not shape a $ZnCys_4$-type site described in other pathogenic bacterial Fur homologs [44].

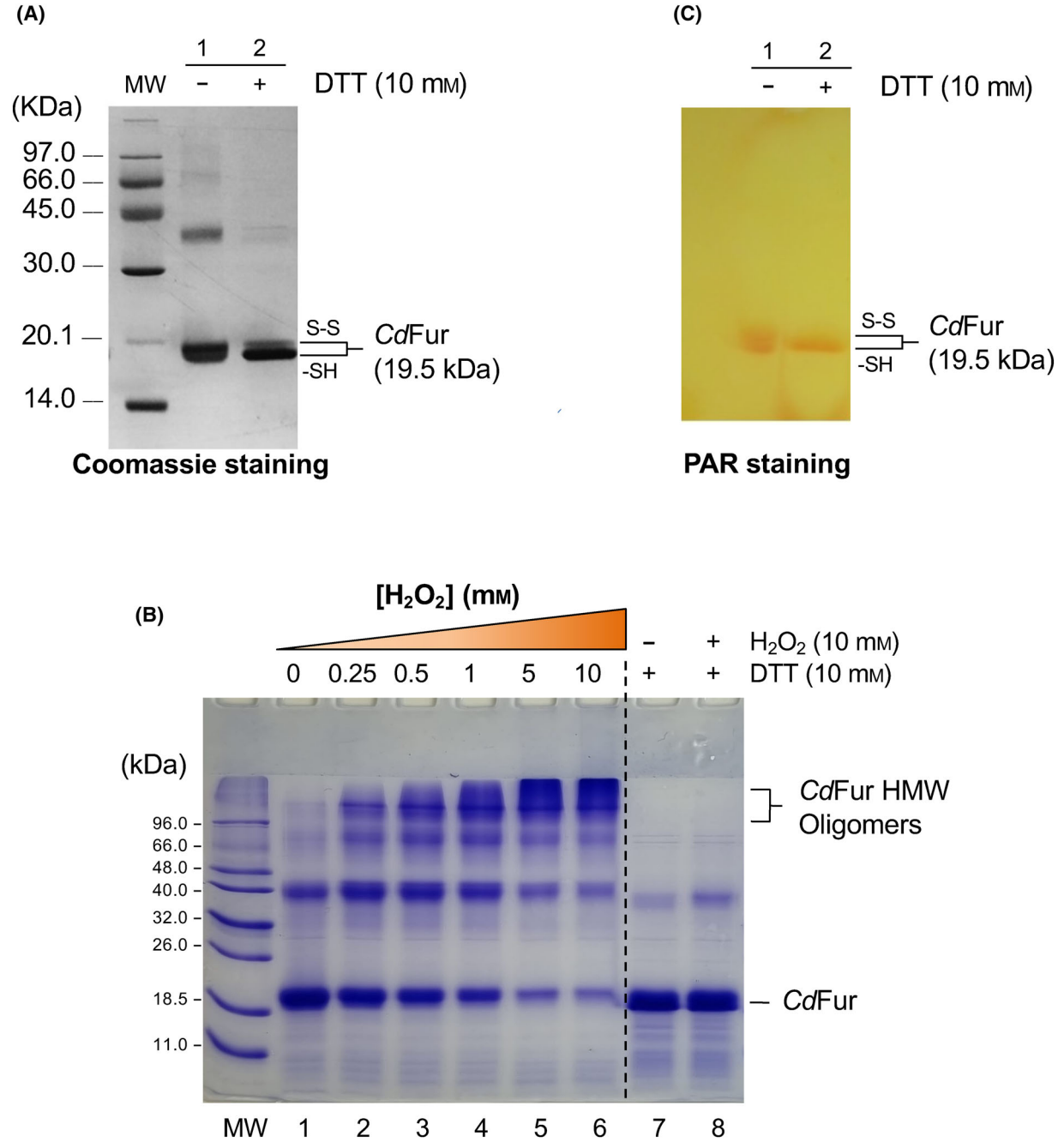

Fig. 4. Electrophoretic mobility of *Cd*Fur visualized on SDS/PAGE gel. (A) 4 μg of *Cd*Fur, as obtained after purification (lane 1) or after 10 min of incubation with 10 mM DTT (lane 2), were resolved on 15% non-reducing SDS/PAGE gel and stained with Coomassie Blue. Lane MW corresponds to protein molecular mass standards. (B) 4 μg of recombinant *Cd*Fur protein was oxidized with increasing amounts of H_2O_2 (0.25, 0.5, 1, 5, 10 mM) for 10 min (lanes 2–6), reduced with 10 mM DTT for 10 min (lane 7), oxidized with 10 mM of H_2O_2 first and then reduced with 10 mM DTT for 10 min (lane 8) or left untreated (lane 1) before 15% non-reducing SDS/PAGE and Coomassie Blue staining. Lane MW corresponds to protein molecular mass standards. Positions of HMW oligomers is indicated on the right. HMW, High molecular weight. The dashed vertical line on the gel has been drawn to facilitate interpretation of the results shown based on the assayed conditions. (C) 4 μg of purified *Cd*Fur without any treatment (lane 1) or after treatment with 10 mM DTT for 10 min (lane 2) were resolved on 15% non-reducing SDS/PAGE gel and stained with PAR for Zn^{2+} ion detection. The shown images in (A), (B) and (C) are representative of three experiments.

Reducing conditions and metal chelator are necessary for *in vitro* DNA binding of *Cd*Fur to target promoter

To determine whether the purified recombinant *Cd*Fur protein was able to bind to DNA in a specific manner, we assayed by gel mobility shift assays (EMSA) different potential target DNA sequences in the presence of a non-specific competitor DNA (P_{nifJ} from the cyanobacterium *Anabaena* sp. PCC 7120). As representative Fur targets, we used the promoter regions of the *fur* (*cd630_1287*), *feoA* (*cd630_1477*) and *fldX* (*cd630_1999*) genes. We selected the first one since the expression of *fur* gene is usually autoregulated [45,46]. The second one encodes a component of a Feo ferrous iron uptake system [47] while *fldX* encodes flavodoxin, a small electron transfer protein that can substitute iron-containing ferredoxin when iron is limited [48]. All these genes had been previously identified as being iron and Fur repressed in *C. difficile* [27]. Unlike Fur proteins from most organisms, we observed that interaction of *Cd*Fur with potential targets only happened under reducing conditions in the presence of the metal chelator EDTA both in the sample buffer and running buffer (Fig. 5A, lanes 2 mM, 10 mM EDTA). An additional control of the binding of *Cd*Fur to its own promoter under reducing conditions (pre-treatment of the protein with 10 mM DTT) in the absence of EDTA showed that reducing conditions hardly promoted the formation of DNA-protein complexes even at higher *Cd*Fur concentration in the binding mixture (Fig. 5B, compare lanes 1–9). When the protein was reduced with DTT, even though it specifically recognized the promoter, very little complex was formed because the binding conditions were not optimal due to the lack of EDTA. Therefore, a slight decrease in the intensity of the P_{fur} band is observed as more and more protein molecules bind to the promoter (Fig. 5B, compare lanes 1–9) but the amount of complex was insufficient to shape a band. Lane 8 in this control experiment (Fig. 5B) confirmed that reducing conditions were insufficient to induce *Cd*Fur to its own promoter and that the presence of EDTA, both in the sample buffer and running buffer, was necessary to observe *Cd*Fur specific binding to target DNA (Fig. 5A, lanes 2 mM, 10 mM EDTA and Fig. 5B, lane 8). Conspicuously, addition of increasing amount of Mn^{2+} to the binding mixture did not promote further binding of the protein to P_{fur} promoter under reducing conditions (Fig. 5A lanes 100, 500, 1000 μM Mn^{2+}). We used divalent metal Mn^{2+} as a surrogate for Fe^{2+} for the *in vitro* analyses of Fur homolog because ferrous iron readily oxidizes to Fe^{3+} in air [49]. Gel mobility shift assays performed under reducing conditions (10 mM DTT) in the presence of EDTA, both in the sample buffer (200 μM) and running buffer (10 mM), showed that the purified recombinant *Cd*Fur protein specifically bound to the three gene promoters P_{fur} (Fig. 6A), P_{feoA} (Fig. 6B) and P_{fldX} (Fig. 6C) in a protein concentration-dependent manner and failed to bind to a competitor DNA lacking Fur boxes (Fig. 6A–C). Thus, according to our results, the addition of divalent metal ions turned out not to be necessary to observe *Cd*Fur DNA-binding activity and the addition of the metal chelating agent EDTA, instead of inhibiting the binding of *Cd*Fur to target promoters, improved it.

Oligomeric *Cd*Fur contains zinc and does not bind to DNA

Based on the results presented so far, it appeared that the interdisulfide mediated species observed in SDS/PAGE under non-reducing conditions remained demetalated, since they were not detected after PAR staining of the gel (Fig. 4C, lanes 1 and 2). Moreover, oxidation of the protein with H_2O_2 led to its oligomerization mediated by disulfide bonds (Fig. 4B, compare lanes 6 and 8). Therefore, we investigated the existence of a possible relationship between *Cd*Fur demetalation and formation of HMW oligomeric species of *Cd*Fur. For this purpose, we determined by ICP-OES the presence of zinc in the oxidized protein. To obtain oxidized *Cd*Fur we treated purified recombinant protein with 10 mM H_2O_2 for 10 min and the reaction product was cleaned up with a PD MiniTrap G-25 column (GE Healthcare, Chicago, IL, USA) to eliminate excess of H_2O_2. We obtained a *Cd*Fur preparation composed mainly by HMW species according to non-reducing SDS/PAGE (Fig. 7, lane 3). No turbidity was observed upon *Cd*Fur oxidation, supporting the notion that HMW oligomeric species previously visualized by SDS/PAGE upon *Cd*Fur oxidation with H_2O_2 were soluble (Fig. 4B, lanes 1–6). Total zinc determination performed by ICP-OES of the oxidized *Cd*Fur preparation indicated that 0.82 ± 0.01 mole of zinc was present per mole of protein, suggesting that formation of *Cd*Fur oligomers produced upon *Cd*Fur oxidation might not involve cysteine residues necessary for zinc coordination. Since, according to EMSA experiments, reducing conditions appeared necessary for optimal binding of *Cd*Fur to target promoters *in vitro*, we analyzed the effect of oxidant conditions on *Cd*Fur DNA-binding ability. Exposure of the recombinant *Cd*Fur protein to 10 mM H_2O_2 rendered a protein preparation that did not show DNA-binding activity *in vitro*, using P_{fur} as DNA target (Fig. 8, lane 2). Controls showing

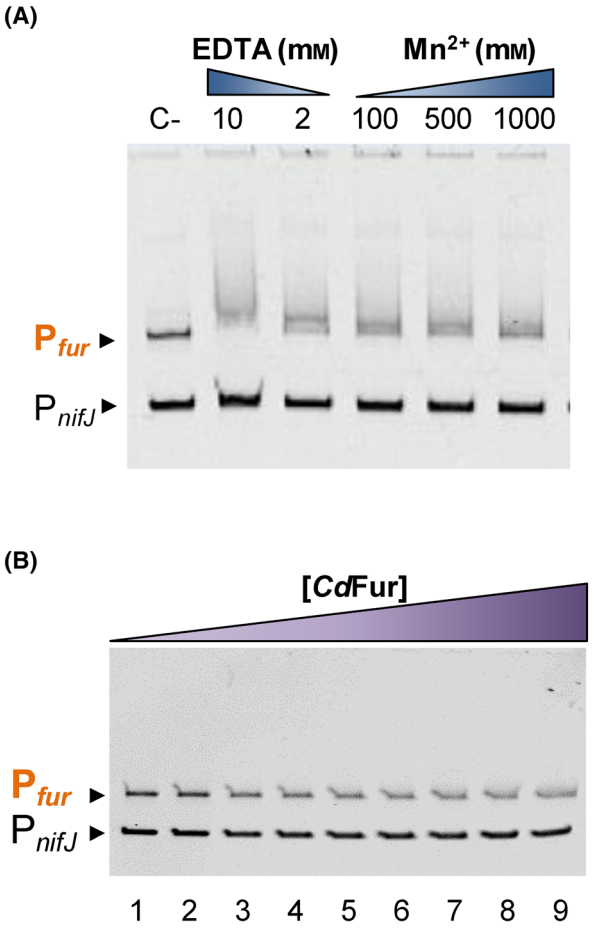

Fig. 5. Effect of metal presence and reducing conditions on *Cd*Fur activity *in vitro* by electrophoretic mobility shift assay (EMSA). (A) Effect of metal (Mn^{2+}) and a chelating agent (EDTA) on the *Cd*Fur activity. 50 ng of P_{fur} was incubated for 30 min with 300 nM *Cd*Fur protein under reducing conditions (10 mM DTT) in binding buffer (20 mM Tris/HCl pH 8, 5 mM KCl, 1 mM $MgCl_2$, 5% glycerol and 0.05 mg·mL^{-1} BSA) and in the presence of EDTA (10 mM or 2 mM) or increasing amounts of Mn^{2+} (100, 500 or 1000 μM). Lane designated 'C-' corresponds to negative control (DNA without protein). Image is representative of three experiments. (B) Effect of DTT on the *Cd*Fur activity. 50 ng of P_{fur} was incubated for 30 min with increasing amounts of purified *Cd*Fur (from 100 nM to 350 nM) (lanes 2–9) under reducing conditions (10 mM DTT) in binding buffer (20 mM Tris/HCl pH 8, 5 mM KCl, 1 mM $MgCl_2$, 5% glycerol and 0.05 mg·mL^{-1} BSA). Lane 1 corresponds to free DNA (without protein) as the negative control and lanes 2 to 9 correspond to the target promoter incubated with 100 nM (lane 2), 125 nM (lane 3), 150 nM (lane 4), 175 nM (lane 5), 200 nM (lane 6), 250 nM (lane 7), 300 nM (lane 8) and 350 nM (lane 9) of *Cd*Fur protein. In all cases, binding reactions were resolved on 6% native polyacrylamide gel. Electrophoresis was performed for 2 h at 90 V with running buffer containing 25 mM Tris/HCl, pH 8 and 190 mM glycine. 50 ng of the promoter region of the *nifJ* gene from the cyanobacterium *Anabaena* sp. PCC7120 were used as non-specific competitor DNA in each binding reaction. Image is representative of two experiments.

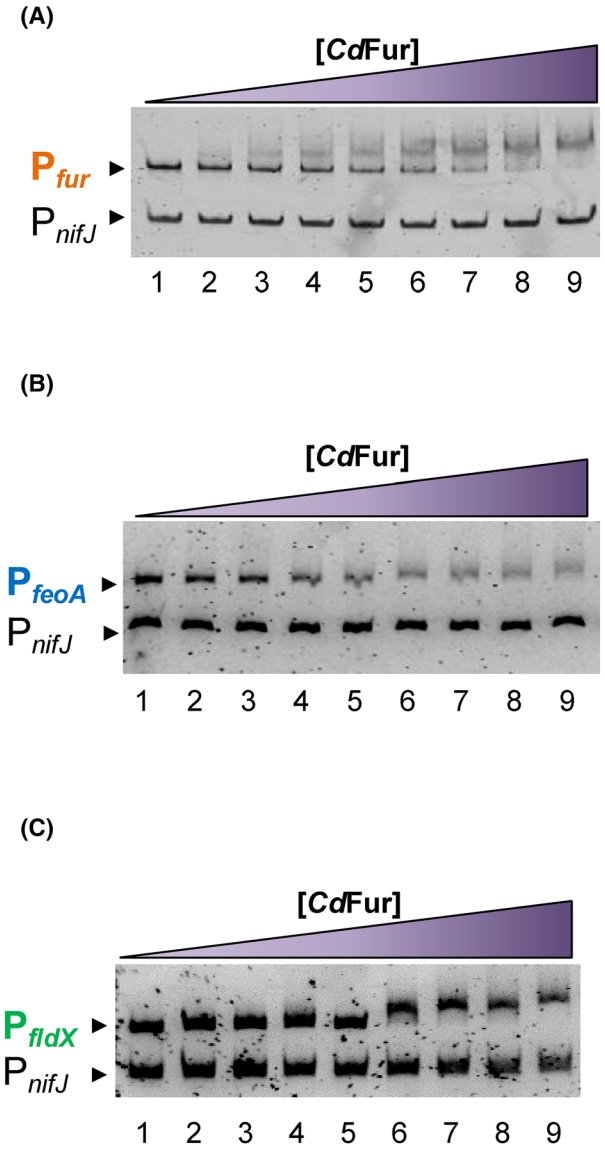

Fig. 6. Binding of *Cd*Fur to *fur*, *feoA* and *fldX* promoters determined by electrophoretic mobility shift assay (EMSA). Selected promoters (50 ng P_{fur} (A), 50 ng P_{feoA} (B) and 50 ng P_{fldX} (C)) were incubated for 30 min with increasing concentrations of recombinant *Cd*Fur (lanes 2–9) in the presence of 10 mM DTT and 200 μM EDTA in binding buffer (20 mM Tris/HCl pH 8, 5 mM KCl, 1 mM $MgCl_2$, 5% glycerol and 0.05 mg·mL^{-1} BSA). Binding reactions were resolved on 6% native polyacrylamide gels. Electrophoresis was performed for 2 h at 90 V with running buffer containing 25 mM Tris/HCl, pH 8, 190 mM glycine and 10 mM EDTA. In gel A, lanes 1 to 9 contained 0, 100, 125, 150, 175, 200, 250, 300 and 350 nM of *Cd*Fur, respectively. In gels B and C, lanes 1 to 9 contained 0, 100, 150, 200, 250, 300, 400, 500 and 600 nM of *Cd*Fur, respectively. 50 ng of the promoter region of the *nifJ* (P_{nifJ}) gene from the cyanobacterium *Anabaena* sp. PCC7120 was used as non-specific competitor DNA in each binding reaction. Images shown in (A), (B) and (C) are representative of three experiments.

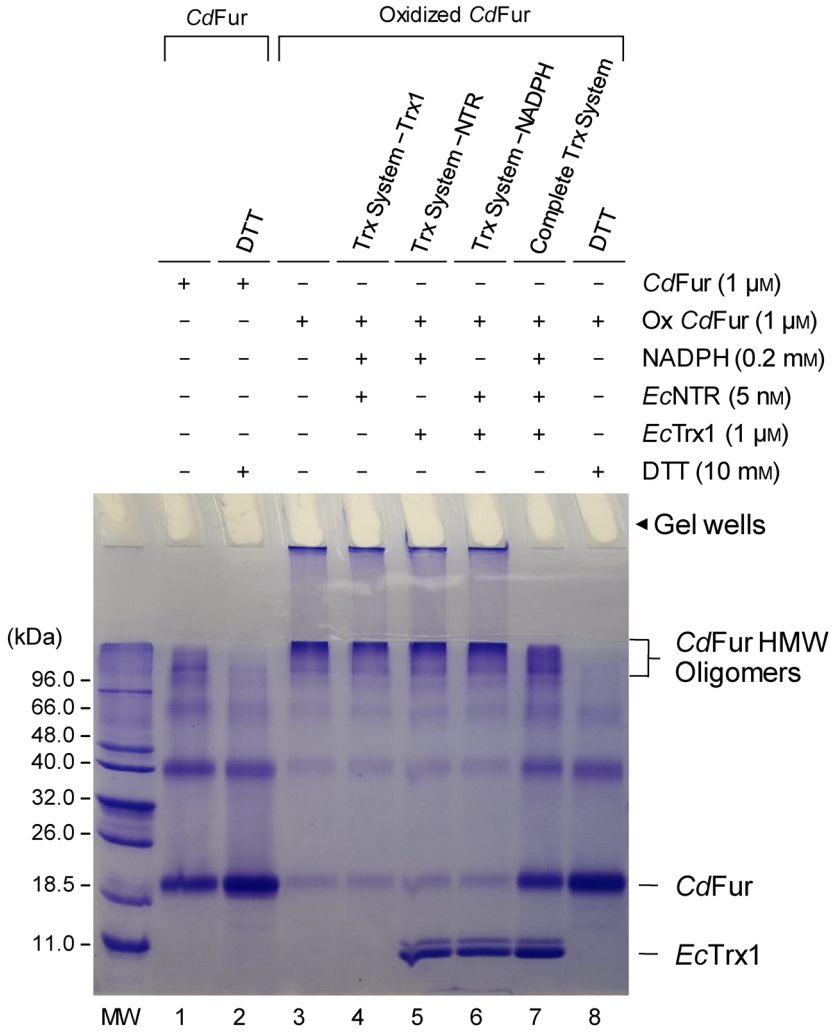

Fig. 7. Reduction of *Cd*Fur by thioredoxin. 1 μM oxidized *Cd*Fur (Ox *Cd*Fur) was incubated at 30 °C for 20 min in 50 mM Tris–HCl pH 8.0, 0.5 mM EDTA with the complete Trx reduction system constituted by 0.2 mM NADPH, 5 nM *Ec*NTR and 1 μM *Ec*Trx1 (lane 7). Controls missing each component of the Trx reduction system [*Ec*Trx1 (lane 4), *Ec*NTR (lane 5) and NADPH (lane 6), untreated Ox *Cd*Fur (negative control, lane 3) and Ox *Cd*Fur reduced with 10 mM DTT (positive control, lane 8)] were also included. In lanes 1 and 2, recombinant *Cd*Fur as obtained after purification (lane 1) and treated with 10 mM DTT (lane 2) were also analyzed. Electrophoresis was performed on 15% non-reducing SDS/PAGE with 5% stacking gel in 0.5 M Tris/HCl pH 6.8 and 15% resolving gel 1.5 M Tris/HCl pH 8.8 and gels were stained with Coomassie Blue. Lane MW corresponds to protein molecular mass standards. The positions of HMW oligomers are indicated on the right. HMW, High molecular weight. The shown image is representative of two experiments.

*Cd*Fur activity treated with DTT and without treatment with this reducing agent are shown in Fig. 8, lanes 1 and 4, respectively. To determine whether the lack of DNA-binding activity observed upon oxidation of *Cd*Fur could be reversed, we treated the oxidized *Cd*Fur with 10 mM DTT and determined its activity by EMSA. Results showed that DNA-binding activity was retrieved after subsequent reduction with DTT of oxidized *Cd*Fur, indicating that the DNA-binding capacity of *Cd*Fur was modulated by redox changes (Fig. 8, lane 3 compared to lane 1).

H_2O_2 boosted *Cd*Fur HMW species are direct substrate of thioredoxin

Intracellular reduction of protein disulfide bridges is mostly performed by thioredoxins and glutaredoxins [50]. The two CXXC motifs in *Cd*Fur resemble the redox active site found in other Fur homologs that have shown to be target for redox-dependent control by thioredoxin [51]. Therefore, we investigated whether the disulfide-mediated HMW oligomeric species obtained after oxidation of *Cd*Fur with H_2O_2 (Fig. 4B, lanes 1–6)

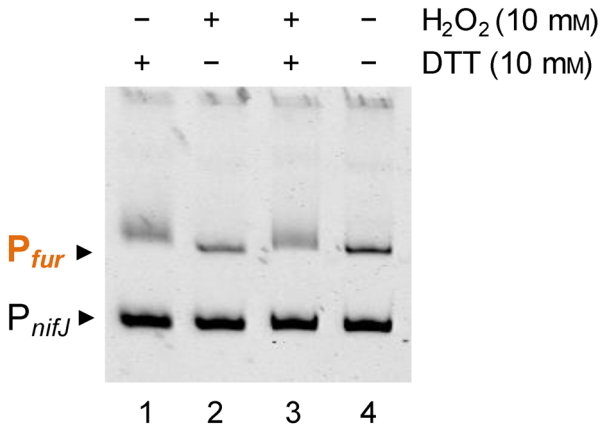

Fig. 8. Oxidation of *Cd*Fur by H_2O_2 leads to reversible *Cd*Fur DNA-binding inactivation. Binding reactions were performed with *Cd*Fur protein samples treated with 10 mM DTT for 10 min (lane 1), 10 mM H_2O_2 for 10 min (lane 2), first with 10 mM H_2O_2 for 10 min and then with 10 mM DTT for 10 min (lane 3) or left untreated (lane 4). 50 ng of P_{fur} was incubated for 30 min with 300 nM *Cd*Fur protein after each of the aforementioned treatments in the presence of 200 μM EDTA in binding buffer (20 mM Tris/HCl pH 8, 5 mM KCl, 1 mM $MgCl_2$, 5% glycerol and 0.05 mg·mL^{-1} BSA). Binding reactions were resolved on a 6% native polyacrylamide gel. Electrophoresis was performed for 2 h at 90 V with running buffer containing 25 mM Tris/HCl, pH 8, 190 mM glycine and 10 mM EDTA. 50 ng of the promoter region of the *nifJ* gene from the cyanobacterium *Anabaena* sp. PCC7120 (P_{nifJ}) was used as a non-specific competitor DNA in each binding mixture. Image is representative of two experiments.

could be reduced by the physiological system consisting of thioredoxin 1 from *E. coli* (*Ec*Trx1) combined with an *E. coli* NADPH thioredoxin reductase, that utilizes NADPH as ultimate reducing power donor (*Ec*NTR) [52]. We used *E. coli* Trx1 to facilitate reduction of oxidized *Cd*Fur since it is a bacterial thioredoxin with low mid-point redox potential (E' = −270/−284 mV) [53]. For this purpose, oxidized *Cd*Fur preparation obtained upon H_2O_2 treatment was incubated with the NADPH→*Ec*NTR→*Ec*Trx1 electron transport chain and the resulting products separated by 15% non-reducing SDS/PAGE electrophoresis. Trx1 was primarily in the oxidized form and treatment of oxidized *Cd*Fur (1 μM) with oxidized *Ec*Trx1 (1 μM) apparently failed to alter the ratio of *Cd*Fur HMW species to monomers compared to the oxidized *Cd*Fur preparation (Fig. 7, lanes 3 and 5, 6). Upon treatment of oxidized *Cd*Fur with reduced *Ec*Trx1 obtained in the presence of NADPH→*Ec*NTR, complete reduction of HMW species that were beyond the migration capacity of the gel was observed (Fig. 7, lanes 3 and 7). Consequently, the protein that remained at the bottom of electrophoresis gel well after running electrophoresis totally vanished, indicating that it was a target of thioredoxin reduction (Fig. 7, lanes 3 and 7). At the same time, there was an increase in the intensity of the band corresponding to the monomer (Fig. 7, lanes 3 and 7), proving the efficiency of reduced thioredoxin to reduce *Cd*Fur HMW species.

Different mixtures of additives and protein tested showed that, in the absence of the complete physiological electron transport system, the ratio of HMW species to monomers was apparently not affected compared to the oxidized *Cd*Fur preparation (Fig. 7, lanes 4, 5, 6 and 7).

Reduced thioredoxin restores sequence-specific DNA binding of oxidized *Cd*Fur

Once it was confirmed that reduced thioredoxin reduces HMW species of *Cd*Fur, we examined the effect of reduced thioredoxin on the DNA-binding activity of oxidized *Cd*Fur using EMSA. We compared the DNA-binding activity of oxidized *Cd*Fur to the *fur* gene promoter in the absence and presence of *Ec*Trx1. As observed in Fig. 9A (compare lanes 5 and 8), *Ec*Trx1 significantly enhanced the sequence-specific binding of *Cd*Fur to the *fur* promoter in the presence of NADPH thioredoxin reductase (*Ec*NTR) and NADPH. If *Ec*Trx1 was absent (Fig. 9A lane 5), *Cd*Fur binding to the *fur* promoter was not observed. This was consistent with results in Fig. 7, lane 4 that showed no reduction of oxidized *Cd*Fur in presence of *Ec*NTR and NADPH when *Ec*Trx1 was absent, indicating that the complete thioredoxin system was necessary to obtain reduced *Cd*Fur (Fig. 7, lane 7). In fact, treatment of oxidized *Cd*Fur with *Ec*Trx1 (200 nM) failed to activate *Cd*Fur (Fig. 9A lane 4), suggesting that *Ec*Trx1 was oxidized. The effect of *Ec*Trx1 was visible to a 1 : 1 enzyme/regulator relation in presence of *Ec*NTR and NADPH and it was equivalent to that of 10 mM DTT in enhancing the *Cd*Fur DNA-binding activity (Fig. 9A compare lanes 8 and 10).

To test whether the effect of thioredoxin observed on *fur* promoter extended to other *in vivo* *Cd*Fur-regulated gene promoters [27], we examined the ability of *Ec*Trx1 to restore the DNA binding of oxidized *Cd*Fur to P_{feoA} and P_{fldX}. We compared the binding capacity of increasing amount of *Cd*Fur to P_{fur}, P_{feoA} and P_{fldX} in the presence and absence of the Trx system (NADPH, *Ec*NTR and *Ec*Trx). Trx system significantly enhanced the DNA-binding ability of oxidized *Cd*Fur to the target promoters (Fig. 9B–D compare lane 2 and lane 5, lane 3 and lane 6 and lane 4 and lane 7, in each gel). The amount of *Cd*Fur needed to observe DNA retardation was lower in the case of the

fur promoter than in the case of *feoA* or *fldX* promoters, suggesting higher affinity of *Cd*Fur for P_{fur} than for P_{feoA} or P_{fldX} promoters. The effect of Trx system on enhancing *Cd*Fur activity was slightly lower to that of DTT at low oxidized *Cd*Fur concentration in the case of the P_{feoA} promoter (Fig. 9C compare lanes 2 and 8) but equivalent to that of 10 mM DTT for the three promoters in the rest of *Cd*Fur concentration values (Fig. 9B–D compare lane 3 and 4 with lanes 8 and 9 respectively in each gel).

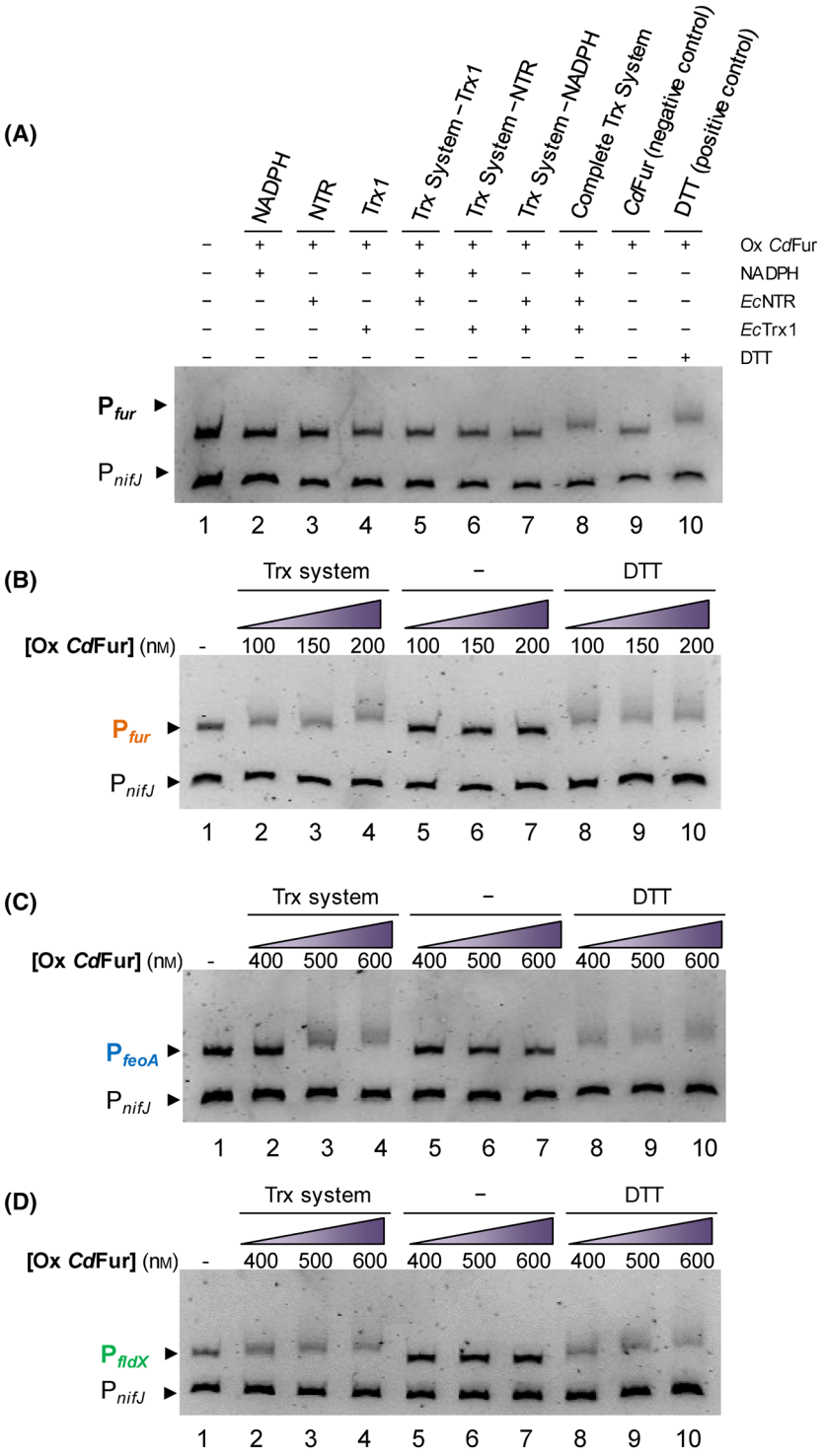

Fig. 9. Influence of reduction by thioredoxin on DNA-binding properties of *Cd*Fur and on the binding to selected target promoters. (A) The effect of the reduction by the Trx system on the DNA-binding activity of oxidized *Cd*Fur was analyzed by EMSA. 50 ng of P_{fur} was incubated with 200 nM of Ox *Cd*Fur (previously incubated with the Trx system, with DTT or left untreated) for 30 min in the presence of 200 μM EDTA in binding buffer (20 mM Tris/HCl pH 8, 5 mM KCl, 1 mM $MgCl_2$, 5% glycerol and 0.05 mg·mL^{-1} BSA). Prior to its addition to the binding reaction mixture, 1 μM of Ox *Cd*Fur was incubated at 30 °C for 20 min with the complete Trx system (1 μM *Ec*Trx1, 5 nM *Ec*NTR, 0.5 mM EDTA and 0.2 mM NADPH) (lane 8). Ox *Cd*Fur was also incubated with the Trx system missing one of the components [*Ec*Trx1 (lane 5), *Ec*NTR (lane 6) and NADPH (lane 7)], and incubated with only one of the components of the Trx system [NADPH (lane 2), *Ec*NTR (lane 3) and *Ec*Trx1 (lane 4)], which served as controls to confirm the need of the complete Trx system (NADPH→*Ec*NTR→*Ec*Trx1) for Ox *Cd*Fur reduction. Reduction of Ox *Cd*Fur with 10 mM DTT was used as a positive control to prove that reduction of oxidized *Cd*Fur allows it to bind to a target DNA promoter (lane 10) whereas untreated Ox *Cd*Fur served as negative control (lane 9). Binding reactions were resolved on 6% native polyacrylamide gels. Electrophoresis was performed for 2 h at 90 V with running buffer containing 25 mM Tris/HCl, pH 8, 190 mM glycine and 10 mM EDTA. 50 ng of the promoter region of the *nifJ* gene (P_{nifJ}) from the cyanobacterium *Anabaena* sp. PCC7120 were used as non-specific competitor DNA in each binding reaction. The effect of DTT and the Trx system on the DNA-binding activity of oxidized *Cd*Fur was analyzed by EMSA using P_{fur} (B), P_{feoA} (C) and P_{fldX} (D) as target DNA promoters. 50 ng of the corresponding promoter was incubated with different concentrations of Ox *Cd*Fur (previously incubated with the Trx system, with DTT or left untreated) for 30 min in the presence of 200 μM EDTA in binding buffer (20 mM Tris/HCl pH 8, 5 mM KCl, 1 mM $MgCl_2$, 5% glycerol and 0.05 mg·mL^{-1} BSA). Prior to its addition to the binding reaction mixture, 1 μM of Ox *Cd*Fur was incubated at 30 °C for 20 min with the complete Trx system (1 μM *Ec*Trx1, 5 nM *Ec*NTR, 0.5 mM EDTA and 0.2 mM NADPH) (lanes 2–4), without any additive (lanes 5–7) or with 10 mM DTT (lanes 8–10). Binding reactions were resolved on 6% native polyacrylamide gels. Electrophoresis was performed for 2 h at 90 V with running buffer containing 25 mM Tris/HCl, pH 8, 190 mM glycine and 10 mM EDTA. 50 ng of the promoter region of the *nifJ* gene (P_{nifJ}) from the cyanobacterium *Anabaena* sp. PCC7120 was used as non-specific competitor DNA in each binding reaction. Each of the shown gel images is representative of two experiments.

fldX and *feoA* gene transcription fluctuates during the *C. difficile* cell growth cycle under iron limitation

According to our experiments of complementation of a *fur* deletion mutant of *E. coli*, *Cd*Fur functions as a holo-repressor *in vivo*, whereas our *in vitro* characterization of the recombinant protein shows that binding of *Cd*Fur to DNA depends on the redox status of some cysteine(s) and does not need metal. In order to clarify this regulation pattern, we tried to find some indication of the existence of both forms of regulation *in vivo*. For this purpose, we used datasets on the transcriptional responses of *C. difficile* to different iron regimes, which are publicly available. We analyzed the evolution of transcription of different genes that have been experimentally demonstrated to be regulated by Fur and iron [27], including *cd630_1477* (*feoA*) and *cd630_1999* (*fldX*), whose promoters have been used as *Cd*Fur targets in the present study. In Fig. 10A, using transcription data obtained by Ho and Ellermeier [27] from Δ*fur vs* wild-type cells grown to mid-log phase under high iron, as well as wild-type cells grown under low-iron *vs* high-iron conditions, we have represented the changes in transcription of these target genes. From the observed changes, a Fur-dependent holo-repression model of regulation for these genes can be inferred. Our *in vivo* *Cd*Fur functionally complementation results are in good accordance with this model. On the other hand, we examined an experimental dataset on the transcriptional response of *C. difficile* to low iron growth conditions obtained by Hastie *et al.* [10] that is available at https://academic.oup.com/femspd/article/76/2/fty009/4830099#supplementary-data. In that dataset, RNAs were obtained at different time points of *C. difficile* growth along iron starvation (early exponential phase of growth, 3 h; mid-log phase of growth, 5 h and late exponential phase of growth, 7 h). As observed in Fig. 10B, the ratio in the transcription of the selected target genes in iron-depleted growth medium *vs* iron sufficient growth medium indicates that they were significantly induced at 3 h (early exponential phase of growth). However, the ratio in the transcription level of these genes underwent an evident reduction at 5 h (mid-log phase of growth) and was strongly induced at 7 h (late exponential phase of growth). The fluctuation in the transcription of these genes along *C. difficile* growth under iron limitation suggests that they experienced repression during exponential phase of growth. This would be compatible with a model of iron independent *Cd*Fur mediated repression of these target genes that would occur in the mean log phase of growth, when iron is scarce, and would correspond to the behavior that we observed for the protein *in vitro*. In addition, it appears that *Cd*Fur would lose affinity for these target promoters in the late exponential phase of growth allowing transcription of these genes. Thus, this analysis suggests that *Cd*Fur might regulate some of its regulon genes both in iron-dependent or independent form according to the iron available during *C. difficile* growth.

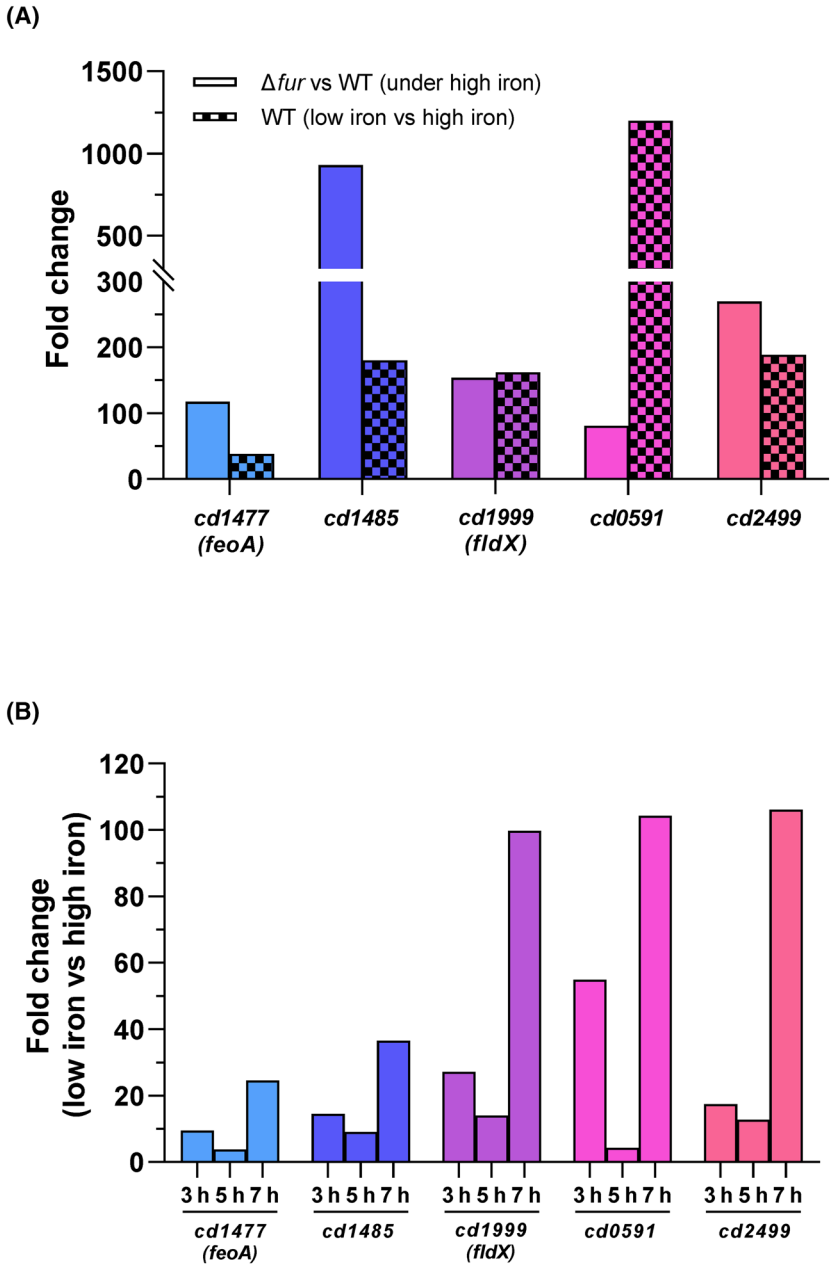

Fig. 10. Analysis of Fur- and iron-dependent regulation of selected *C. difficile* genes. (A) Analysis of Fur and iron repression of selected *C. difficile* genes. For each gene, the fold change of Δ*fur* under high iron *vs* WT under high iron and the fold change of WT under low iron *vs* high iron is represented. Data used in this panel were obtained from table 3 of Ho and Ellermeier [27]. Samples used for microarray analysis were obtained from the *C. difficile* wild-type and/or Δ*fur* mutant grown to mid-log phase in high- or low-iron-containing growth medium. (B) Evolution of fold changes during iron starvation of selected *C. difficile* genes that are repressed by *Cd*Fur under iron sufficiency. Transcriptomic data used to elaborate this panel were taken from Supplementary Material of Hastie *et al.* [10]. For each gene, the fold change (ratio of transcription in iron-depleted growth medium to iron-sufficient growth medium) at different time points during *C. difficile* growth under iron starvation is represented. These time points represent the time elapsed from the beginning of the growth curve and correspond to different stages of the exponential growth phase (3 h: early-log phase; 5 h: mid-log phase; 7 h: late-log phase). The phases of bacterial growth were identified using the growth curve shown in Fig. 1 of the same reference [10]. The genes analyzed in this panel were selected from table 3 of Ho and Ellermeier [27].

Discussion

Despite the apparent importance of the ferric uptake regulator in the control of different aspects of *C. difficile* physiology to adapt vegetative cells to stress conditions imposed by the host [54,55], little is known about its mechanism of functioning. Ho and Ellermeier [27] demonstrated Fur and iron-dependent repression of genes encoding several putative cation transporters of different classes *in vivo* and they verified by EMSA that Fur functioned as a repressor of the *feo*A gene (*cd1477*). However, in these assays, they used Fur protein synthesized by *in vitro* transcription and translation, since the expression of N-terminally His-tagged Fur protein rendered inactive preparations [27].

In the present study, we have successfully purified active recombinant *Cd*Fur from *E. coli* and analyzed its biochemical and functional characteristics, revealing aspects of its regulatory capacity that go beyond its function as a holo-repressor. The results herein demonstrate that recombinant expression of *Cd*Fur in *E. coli* complements Fur deficiency of the mutant host. Thus, recombinant *Cd*Fur is active *in vivo* and it down-regulates the expression of the heterologous *fiu* gene in an iron-dependent manner, as previously reported for other Fur homologs [56]. Hence, *Cd*Fur is able to specifically recognize and bind to iron boxes from *E. coli* promoters, suggesting a high homology in both structure and mechanism of action of both regulators.

Unexpectedly, in contrast to the *in vivo* results, addition of metal co-regulator in the *in vitro* binding assays does not stimulate recombinant *Cd*Fur specific binding to its target promoters. Furthermore, presence of the metal chelating agent EDTA in the *in vitro* binding assays enhances the DNA-binding ability of the recombinant *Cd*Fur for its target promoters. A similar behavior has been reported for the Fur homolog from *Listeria monocytogenes* which does not require iron or manganese ions to bind to *fur* or *fhuDC* gene promoters in EMSA assays. Besides, its ability to bind to these promoters is not inhibited by 2 mM EDTA, although *in vivo L. monocytogenes fur* is autoregulated in response to iron [46].

In the case of recombinant *Cd*Fur, binding to its target promoters under reducing conditions in the absence of metal is dependent on protein concentration (Fig. 6A–C, lanes 1 to 9). This last behavior has been described for Fur of *H. pylori* [21,57,58] and *C. jejuni*, [25] and, in particular, expression of two of the Fur targets in *H. pylori* (*sodB* and *pfr*) appeared repressed when iron was limited. However, we have found a significant difference between *C. difficile* and *H. pylori*. Whereas the apo-Fur regulon in *H. pylori* was predicted to contain 16 target genes not included in the holo-regulon of Fur [59,60], in the case of *C. difficile* previous published *in vivo* studies [27] and our own *in vitro* results (Fig. 6A–C) indicate that *Cd*Fur can recognize *feo*A, *fldX* promoters or *fur* own promoter in both, presence and absence of metal.

To clarify the regulation pattern of Fur in *C. difficile*, we correlated our *in vitro* results with previous findings in terms of transcriptional regulation. As *Cd*Fur does not need metal under reducing conditions to be functional *in vitro*, we examined published data on the transcriptional response of *C. difficile* throughout growth under iron starvation that are publicly available in order to find some indication of the possible existence of *Cd*Fur mediated transcription independent on iron [10,28]. We found that some genes, previously shown to be repressed by Fur and iron in a holo-repression manner, e.g. *cd630_0591* (encoding cation transporting ATPase), *cd630_1999* (encoding flavodoxin) or *cd630_1477* (encoding ferrous iron transport protein FeoA), among others [27] (Fig. 10A), were induced in the early exponential phase of growth, their transcription levels underwent a significant reduction during the mid-log phase of growth and they were strongly induced in the late exponential phase of growth (Fig. 10B) [10]. The evolution observed in the transcription level of these genes indicates that they experienced repression during exponential phase of growth under iron deficiency, suggesting that *Cd*Fur would repress these genes in the mean log phase of growth, when iron is scarce without the need of using iron as corepressor. It should be noted that this growth phase cannot be differentiated in a plate culture maintained at 37 °C for 16–18 h, as the one shown in Fig. 1. Therefore, despite the result observed on the -Fe^{2+} plate shown in Fig. 1, where *Cd*Fur appears inactive in the absence of iron, possible repression by this regulator independent of iron in the mid-log phase of growth cannot be ruled out since there is no certainty that the result observed in that plate corresponds to a culture in the mid-logarithmic phase of growth. Experimental data obtained by Berges *et al.* [28] would also support similar repression as the one we propose for these genes. These authors compared transcriptomic data (RNA-Seq) from samples of wild-type and the *fur* mutant grown under iron limiting growth conditions (0.2 μM) with samples of iron saturated (15 μM) growth conditions. In these studies, samples for RNA isolation were obtained at the mid-exponential phase of growth. This phase of *C. difficile* growth coincides with the phase growth

(5 h) where significant reduction in the transcription level of *feoA* is observed under limited iron conditions according to Hastie *et al.* results used to generate Fig. 10B. Curiously, in Berges *et al.* results none of the FeoA type systems were found more abundant at the transcriptome level with 0.2 μM iron, as low iron conditions. Thus, there seems to be a similarity between the two studies regarding the reduction in the transcription of the *feoA* gene in the same growth phase when there is iron limitation. On the contrary, the strong derepression experienced by *cd630_0591*, *cd630_1999* and *cd630_1477* genes in the late exponential phase of growth (Fig. 10B) would indicate that under these growth conditions, *Cd*Fur is released from these gene promoters. Interestingly, also in the late-log phase of growth the genes of two proteins involved in mitigating uncontrolled protein oxidation, namely thioredoxin 2 (*trxA2*, *cd630_2355*) and thioredoxin reductase 3 (*trxB3*, *cd630_2356*), were induced in the iron-depleted culture [10]. This would support the notion that *C. difficile* could experience oxidative stress under iron deficiency. In fact, a recent study evaluating the transcriptional response of two *C. difficile* strains (630 and CD196) to long-term 1.5% oxygen exposure showed that the *trxA2* gene was induced in CD630 strain in response to oxidative stress [29]. Therefore, these observations point to iron deficiency leading to oxidative stress in *C. difficile* cells in the late exponential phase of growth. Indeed, iron limitation appears to be a cause of endogenous oxidative stress in bacterial cells as reported in the cyanobacterium *Anabaena* sp. PCC 7120 or in the alphaproteobacterium *Caulobacter crescentus*. In *Anabaena* cells, iron starvation leads to a significant increase in reactive oxygen species [61] and *C. crescentus* in iron-limited media presents a higher amount of endogenous H_2O_2 [62].

On the other hand, our results clearly demonstrate that *Cd*Fur is subjected to redox control and responds to oxidative stress *in vitro*. First, recombinant *Cd*Fur forms disulfide-mediated high-order weight species by H_2O_2 in a dose-dependent manner (Fig. 4B lanes 1–6), which is sufficient to avoid *Cd*Fur binding to the analyzed *cd630_1287* (*fur*), *cd630_1999* (*fldX*) and *cd630_1477* (*feoA*) gene promoters (Fig. 9B–D lanes 5, 6 and 7 in each gel). Second, reducing conditions revert the protein oligomerization process (Fig. 7 compare lanes 3 and 8), which in turn promote *Cd*Fur binding to DNA (Fig. 9B–D, compare lanes 5, 6 and 7 with lanes 8, 9 and 10 in each gel). Third, and relevantly, the reversal in the oligomerization state and consequent activation of *Cd*Fur is achieved not only with a reducing chemical system (DTT) but also with a biological one (Fig. 9B–D, lanes 2, 3 and 4). In this sense, we have demonstrated that a complete Trx reductase/Trx system reduces *Cd*Fur HMW species obtained upon oxidation of *Cd*Fur with H_2O_2 (Fig. 7 compare lanes 3 and 7) and the reduction product binds to *fur*, *feoA* or *fldX* promoters (Fig. 9B–D, lanes 2, 3 and 4 in each gel). Thus, although it is always difficult to extrapolate findings in an *in vitro* system to *in vivo* bacterial physiology, from our *Cd*Fur biochemical characterization and from the analysis of published transcription data a model of *Cd*Fur functioning under iron limitation could be proposed. We envisage that the increase in the transcription of *fldX* or *feoA* genes observed in *C. difficile* cultures that have reached the late exponential phase of growth under iron limitation compared with their transcription level observed in the mid-exponential phase of growth [10] would be a consequence of the loss of affinity for DNA underwent by *Cd*Fur after oligomerization under oxidative stress conditions generated by iron deficiency. Once inactivated by oligomerization, *Cd*Fur would revert to its DNA-binding competent status upon reduction by a Trx reductase/Trx system (Fig. 11). Accordingly, formation of *Cd*Fur HMW oligomers by means of one or more disulfide bonds might be an additional regulatory mechanism to control *Cd*Fur binding to target promoters under exposure to oxidizing conditions. Although the model of *Cd*Fur DNA-binding activity based on oxidation/reduction transitions we propose is obtained from *in vitro* results, a thiol redox proteomics approach on micro-aerobically shocked *C. difficile* cells indicated that some peptides that underwent increase in the oxidative state of cysteines after 15 min of micro-aerobic shock belonged to Fur, suggesting that indeed this regulator contains cysteine residues that are prone to oxidation *in vivo* [63].

Control of Fur activity by a thiol-based redox switch has been described previously for the FurA homolog from *Anabaena* sp. PCC7120 [26]. In this case, formation of one intramolecular disulfide bond affects the redox state of one cysteine residue that is part of a conserved CXXC motif and is responsible for the protein ability to coordinate the metal corepressor and hence to bind to DNA. In other Fur homologs, these CXXC motifs are involved in coordination of a structural zinc atom [24,25]. Although *Cd*Fur includes two CXXC motifs ($C_{101}XXC_{104}$ and $C_{141}XXC_{144}$) in its primary structure (Fig. 2) and it seems to contain one tightly bound zinc atom per protein monomer, both CXXC motifs do not appear to be simultaneously involved in the binding of this metal. Neither does it appear that coordination of zinc in *Cd*Fur may involve cysteines of the redox switch

since *Cd*Fur experienced oligomerization by disulfide bond formation under oxidizing conditions, but oxidation did not affect zinc contents of the protein. Therefore, the presence of zinc may have a stabilizing function of the protein architecture, as reported for *E. coli* Fur [64]. In order to characterize the *Cd*Fur redox switch, work is now underway to determine which of the seven cysteine residues of *Cd*Fur are involved in redox state sensing and if some of them participate in zinc coordination.

Finally, our study points to a redox control of *Cd*Fur binding to target promoters under iron limitation that is independent of iron. However, these same target promoters are controlled by *Cd*Fur in an iron-dependent manner under iron sufficiency [27]. To make compatible both regulatory aspects by *Cd*Fur, the possibility arises that the regulation of some genes by Fur in this anaerobic pathogen in response to an increase in intracellular free iron is based on *Cd*Fur ability to associate with some iron-containing prosthetic group instead to mononuclear iron. Recently, Lill [65] proposed that it might not be mononuclear Fe^{2+} but an iron cluster that serves as iron regulatory device in Fur. This proposal was based on Fontenot *et al.* [66] results showing that Fur purified from *E. coli* binds an all-Cys coordinated [2Fe-2S] cluster. In fact, binding of a [2Fe-2S] in response to elevation of intracellular free iron content has been already shown for the Fur homologs of *Vibrio cholerae* and *H. pylori*, although demonstration of the binding of these [2Fe-2S]-containing Fur proteins to target promoters has not been reported [67]. Though still tentative, it could be the case that *Cd*Fur senses the iron level via iron cluster occupancy. Thus, it cannot be ruled out that the *Cd*Fur population exerting its repressing function in the corresponding plate in Fig. 1 is associated to a prosthetic group, rendering a protein population with structural differences with the recombinant *Cd*Fur protein that we have biochemically and functionally characterized, which lacks any prosthetic group. Curiously, during recombinant *Cd*Fur purification process, a band of intense purple color was

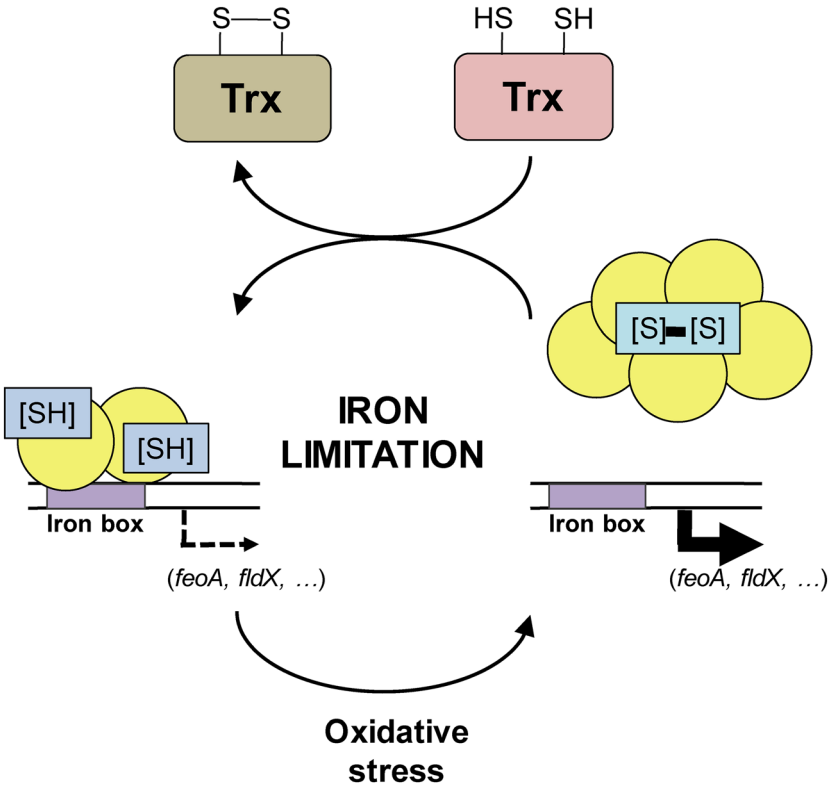

Fig. 11. Proposed model for the regulation of *Cd*Fur DNA-binding activity under iron limitation by a thiol-disulphide redox switch. *Cd*Fur HMW oligomers by means of one or more disulfide bonds are formed under oxidizing conditions, with concomitant transcription of target genes. Once inactivated by oligomerization, *Cd*Fur may revert to its DNA-binding competent status upon reduction by a Trx reductase-Trx system leading to repression of target genes. Brackets indicate that one or more disulphide bonds may be involved. HMW, High molecular weight. The dashed promoter arrow indicates a lower level of transcription than the undashed promoter arrow.

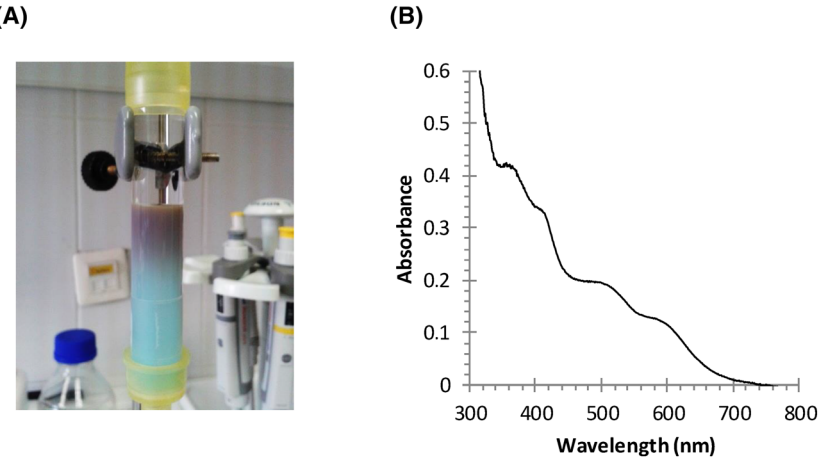

Fig. 12. Purification of *Cd*Fur. (A) Ni-NTA resin after washing the fixed protein extract with 50 mM Tris/HCl buffer containing 45 mM imidazole and 500 mM NaCl at pH 8. (B) UV spectrum of the fraction with the highest color eluted from the Ni-NTA resin using an imidazole gradient from 45 mM to 1 M in 50 mM Tris/HCl buffer containing 500 mM NaCl at pH 8. The UV spectrum is representative of two independent protein preparations.

observed on top of the IMAC chromatographic matrix after crude extract fixation (Fig. 12A). We recovered colored fractions from the chromatographic column but the UV spectrum of the harvested fraction with the highest color could not be associated to the presence of a 2Fe-2S group or any other prosthetic group (Fig. 12B). Taking into account that fraction color vanished in a short time and that recombinant protein UV spectrum lacked any absorbance in the visible region of the spectrum, it is possible that *Cd*Fur binds to an oxygen-sensitive iron cluster. In this way, the UV–visible spectrum we measured could correspond to a mixture of different holo-protein redox species. Additional experiments are required to explain all these observations and to demonstrate whether *Cd*Fur bound to an iron cluster is responsible for the holo-repression described *in vivo* and observed in our *E. coli* Fur-deficient strain complementation assay (Fig. 1). If confirmed, the binding characteristics of *Cd*Fur observed both *in vivo* and *in vitro* for *fur*, *feoA* and *fldX* promoters would be reminiscent from that shown by IscR, the transcriptional regulator of Fe-S biogenesis in *E. coli*. In this case, either [2Fe-2S]-IscR and IscR-C92A/C98A/C104A, a mutant that lacks the cluster, bind to the *hyaA* gene promoter with similar apparent K_d indicating that binding of the regulator to the *hyaA* gene promoter is not dependent on cluster occupancy [68].

In conclusion, this work expands our knowledge of the Fur-dependent transcriptional regulation. We describe a reversible inactivation/activation mechanism dependent on oligomerization for a Fur homolog, which responds to oxidizing conditions and is modulated by thioredoxin. Moreover, our study suggests that Fur from *C. difficile* could control some of its regulon genes both in presence and absence of corepressor metal, hinting an additional Fur-mediated mechanism of *C. difficile* to adapt to low iron environments. Finally, this study contributes to a better understanding of how *C. difficile* might keep iron homeostasis in the iron limited conditions that it faces during infection [27] and how it could mediate oxidative stress response.

Materials and methods

Bacterial strains and growth conditions

Escherichia coli strains used in this study are listed in Table S1. DH5α strain was used as standard competent cells for general cloning procedures and BL21 (DE3) strain was used for protein expression and purification. *E. coli* strain H1780 [33] was used for *Cd*Fur complementation assay. For routinely cultures, all strains were grown aerobically on solid or liquid Luria-Bertani (LB) medium at 37 °C. When necessary, growth media were supplemented with kanamycin (Km, 50 $\mu g \cdot mL^{-1}$) and/or chloramphenicol (Cm, 30 $\mu g \cdot mL^{-1}$).

General manipulations of DNA

PCR products were purified using QIAquick PCR Purification Kit (Qiagen, Germantown, MD, USA). Rapid isolation of plasmid DNA was done using GenElute™ Plasmid Miniprep Kit (Sigma-Aldrich, St. Louis, MO, USA) according to the manufacturer's instructions. Restriction enzymes (Thermo Scientific, Waltham, MA, USA), T4

DNA ligase (Promega) and high-fidelity *Pfu* ULTRA DNA polymerase (Agilent, Santa Clara, CA, USA) were used according to the manufacturer's specifications.

Cloning procedures

The plasmids constructed in this study are listed in Table S1 and the primers used are listed in Table S2. All cloning were performed using the genomic *Clostridium difficile* ATCC 43255 DNA. To overexpress the *C. difficile* Fur protein, the ORF *fur* gene (UAB_RS0207325/a 429 bp DNA fragment) was amplified by PCR with primers Cdfur_up and Cdfur_dw. The forward primer Cdfur_up encoded a NdeI restriction site and the reverse primer Cdfur_dw encoded a HindIII restriction site. The PCR product was digested with appropriate restriction enzymes and was inserted into the expression vector pET28a(+) (Novagen, Merck, Darmstadt, Germany) to generate pET-*Cd*fur, which allowed protein expression with a N-terminal His-tag. The same procedure was used to create the plasmid pACYC-*furCd* using instead the reverse primer Cdfur_dw2 encoding a XhoI restriction site. For this purpose, the ORF *fur* gene properly amplified and digested was introduced into the pACYCT2 vector (Addgene, Watertown, MA, USA; plasmid # 45799).

Complementation of *Cd*Fur in a fur-deficient *E. coli* strain

The *fur*-negative *E. coli* indicator strain H1780, harboring the *fiu*::*lacZ* reporter fusion, was used for the functional complementation assay. *fiu* is an iron-inducible Fur-repressible promoter in *E. coli*. The activity of the β-galactosidase reporter gene was monitored by reading color of colonies on MacConkey agar (Panreac Química S.L.U., Barcelona, Spain). Agar plates were supplemented with 100 μM $FeCl_3$ or with 200 μM of the iron chelator 2,2′-dipyridyl (Sigma-Aldrich) to achieve iron-replete or iron-limited conditions, respectively. The introduction of the *C. difficile* Fur homolog into H1780 competent cells was performed by transformation with pACYC-*furCd* plasmid. The expression of the *Cd*Fur protein was induced by addition of isopropyl β-D-1-thiogalactopyranoside (IPTG, AppliChem GmbH, Darmstadt, Germany) to a final concentration of 1 mM and cells were grown in LB medium until mid-log phase. The cultures were inoculated on MacConkey agar plates and were incubated for 18–24 h at 37 °C. *E. coli* H1780 without plasmid was used as negative control.

Overexpression and protein purification

Vector pET-*Cd*fur was transformed into *E. coli* BL21 (DE3) cells for protein expression. Overnight cultures of *E. coli* BL21 (DE3) transformants were diluted 100-fold in fresh LB broth supplemented with 50 $\mu g \cdot mL^{-1}$ Km and 1 mM IPTG was added when cultures reached OD_{600} of ~ 0.6. Cells were grown for another 3 h and were then harvested by centrifugation and resuspended in 50 mM Tris/HCl pH 8, 500 mM NaCl, 20 mM imidazole, 1 mM PMSF. After lysis by sonication on ice and cell debris removing by centrifugation, protein was purified by nickel iminodiacetic acid (Ni-IDA) affinity chromatography (GE Healthcare). Elution of recombinant protein was performed increasing the concentration of imidazole from 20 mM to 1 M using a gradient maker. Purified *Cd*Fur was dialysed in 50 mM Tris/HCl pH 8, 150 mM NaCl, 10% (v/v) glycerol and stored at −20 °C. Protein concentration was determined spectrophotometrically using the theoretical extinction coefficient ($\varepsilon_{280\ nm} = 7825\ M^{-1}\ cm^{-1}$) or by BCA Protein Assay (Pierce™ BCA Protein Assay Kit, Thermo Scientific, Rockford, IL, USA), according to the manufacturer's instructions. Removal of N-terminal His-tag from the recombinant protein was performed after treatment of 10 mg of *Cd*Fur with 1 U of thrombin overnight at room temperature, according to the manufacturer's instructions.

To obtain oxidized *Cd*Fur (Ox *Cd*Fur), recombinant protein was oxidized for 15 min using 10 mM of H_2O_2, which was removed after treatment using a PD MiniTrap G-25 column following manufacturer's instructions.

Escherichia coli NTR and Trx1 were obtained as described in Buey *et al.* [52]. Briefly, *E. coli* NTR and Trx cloned in pTEV5 plasmid served to produce recombinant proteins containing a His-tag in Rosetta (DE3) *E. coli* cells. Both proteins were purified using Ni^{2+} HiPrep affinity chromatography, the tag was removed by a His-tagged TEV protease and, in the case of NTR, the protein was incubated with an excess of FAD. Both proteins were further purified by gel filtration using a Sephacryl S-300 HR column (Cytiva, Barcelona, Spain) equilibrated in 20 mM Tris/HCl pH 7.6, 150 mM NaCl and 2 mM β-mercaptoethanol.

Spectroscopic analyses

Ultraviolet–visible (UV–vis) absorption spectra were recorded on a Cary 100 UV–Vis double beam spectrophotometer (Agilent Technologies). Far-UV circular dichroism spectrum of 20 μM *Cd*Fur protein was collected on a Chirascan spectropolarimeter (Applied Photophysics Ltd., Surrey, UK). Spectrum was acquired in a 1-mm-path-length cell at room temperature from 200 to 250 nm. A pure solvent baseline was measured with the same cell and subtracted. The molar ellipticity ([θ]) was expressed in $deg \cdot cm^2 \cdot dmol^{-1}$.

Matrix-assisted laser desorption/ionization time of flight mass spectra were recorded with a 4800 plus MALDI-TOF/TOF™ Analyzer (Applied Biosystems, Thermo Fisher Scientific, Waltham, MA, USA; Servicio de Proteómica Instituto Aragonés de Ciencias de la Salud, Spain). 100 μL of 50 μM *Cd*Fur in 20 mM Tris/HCl pH 8, 15 mM NaCl, 1% (v/v) glycerol were used for experimental analyses.

SDS/PAGE sample preparation and analysis

To study the effect of reduction or oxidation on *Cd*Fur oligomerization, *Cd*Fur was incubated for 10 min at room temperature with increasing quantities of H_2O_2 (0.25, 0.5, 1, 5, and 10 mM), with 10 mM DTT or with both (first incubated with 10 mM H_2O_2 and then with 10 mM DTT).

To assess whether *Ec*Trx1 was able to revert *Cd*Fur oligomerization, the electron transport chain *Ec*Trx1 → *Ec*NTR → *Cd*Fur was reconstructed *in vitro* following the procedure described in Guío *et al.* [51]. 1 μM of Ox *Cd*Fur was incubated with 1 μM of *Ec*Trx1, 5 nM of *Ec*NTR and 0.2 mM NADPH in a final volume of 400 μL of 50 mM Tris/HCl pH 8.0, 0.5 mM EDTA. Ox *Cd*Fur was also incubated with the Trx system missing one of its components (NADPH, *Ec*NTR, or *Ec*Trx1) as a negative control and with 10 mM 1,4-dithiothreitol (DTT) as a positive control for protein reduction. After incubation for 20 min at 30 °C, proteins were precipitated with 10% (w/v) trichloroacetic acid (TCA) for 15 min on ice and centrifuged at 8000 ***g*** for 10 min at 4 °C. Pellets were washed with cold acetone and precipitates were resuspended in 20 μL of 50 mM Tris/HCl pH 8.0, 1% (w/v) SDS.

All samples were mixed with Laemmli buffer without β-mercaptoethanol and subjected to 15% non-reducing SDS/PAGE. Gels were stained with Coomassie Blue and destained to visualize the proteins.

Electrophoretic mobility shift assays

Electrophoretic mobility shift assays (EMSAs) were performed to evaluate the DNA-binding activity of the purified protein *in vitro*. All promoters (P_{fur}, P_{feoA} and P_{fldX}) were amplified from *C. difficile* 630 genomic DNA using the primer pairs listed in Table S2. For the negative control, the promoter of *nifJ* gene from *Anabaena* sp. PCC7120 was amplified from *Anabaena* genome using primer pairs listed in Table S2.

All experiments were carried out by incubating *Cd*Fur with 50 ng of the promoter region of interest and 50 ng of P_{nifJ} in 20 μL of binding buffer [20 mM Tris/HCl pH 8, 1 mM $MgCl_2$, 5 mM KCl, 0.05 mg·mL^{-1} bovine serum albumin and 5% (v/v) glycerol] for 30 min at room temperature. After incubation, 3 μL of loading buffer [binding buffer containing 50% (v/v) glycerol and 0.002% bromophenol blue] were added to each sample and samples were loaded onto a 6% non-denaturing PAGE gel. Gel electrophoresis was performed in buffer containing 25 mM Tris/HCl pH 7.4 and 190 mM glycine for 2 h at 90 V and 4 °C. Gels were stained with SYBR® Safe (Invitrogen, Carlsbad, CA, USA) and visualized in a Gel-Doc 2000 device (Bio-Rad). When necessary, EDTA was incorporated both in electrophoresis buffer (10 mM) and in the reaction mixture buffer (200 μM, 2 mM or 10 mM). Besides, depending on the tested conditions, DTT (10 mM), H_2O_2 (10 mM), Mn^{2+} (100 μM, 500 μM or 1 mM) were added to binding reaction mixtures.

To assess the effect of the reduction by *Ec*Trx1 on the DNA-binding activity of oxidized *Cd*Fur, prior to its addition to the binding reaction mixture, Ox *Cd*Fur was incubated with the electron transport chain *Ec*Trx1 → *Ec*NTR → *Cd*Fur as described before (1 μM of Ox *Cd*Fur was incubated with 1 μM of *Ec*Trx1, 5 nM of *Ec*NTR, and 0.2 mM NADPH in a final volume of 100 μL of 50 mM Tris/–HCl pH 8.0, 0.5 mM EDTA for 20 min at 30 °C). Controls incubating Ox *Cd*Fur with 10 mM DTT or removing some of the components of the Trx system were also performed.

Metal content analysis

To remove metal ions from the purified protein, *Cd*Fur in 50 mM Tris/HCl pH 8, 150 mM NaCl and 10% (v/v) glycerol were treated with 10 mM EDTA overnight at 4 °C. To remove extra EDTA, PD-10 desalting columns equilibrated with 50 mM Tris/HCl pH 8, 150 mM NaCl and 10% (v/v) glycerol were used and two additional dialysis in the same buffer were performed. The metal content of the fresh purified protein and after treatments with EDTA, as well as of the oxidized protein (Ox *Cd*Fur), were analyzed using ICP-OES at Ionomics Service of CEBAS-CSIC (Spain). Measurements were carried out in triplicate.

On-gel Zn^{2+} detection

*Cd*Fur (4 μg) was treated with 10 mM DTT or 10 mM H_2O_2 for 10 min and samples were resolved on non-reducing 15% SDS/PAGE gels. The SDS/PAGE gel was soaked in 25 mM Tris/HCl pH 8, 75 mM NaCl, 5% (v/v) glycerol and 500 μM 4-(2-pyridylazo) resorcinol (PAR, Sigma-Aldrich) for 2 min, and subsequently 50 mM H_2O_2 was added to release Zn^{2+}. A photograph of the gel was taken within 10 min of the addition of peroxide due to the light-orange color transient development.

DTNB assay for free thiol determination

The free thiol content of *Cd*Fur was determined by using the Ellman's reagent [69], [5,5′-dithiobis-(2-nitrobenzoic acid)] (DTNB; Sigma-Aldrich). Briefly, 10 μM *Cd*Fur was modified with 100-fold molar excess of DTNB at 25 °C for 20 min under denaturing conditions (6 M guanidinium chloride). Formation of thionitrobenzoic acid was monitored over time at 412 nm by using an extinction coefficient of 13 600 M^{-1}·cm^{-1}.

Bioinformatic tools

The sequence of Fur from *C. difficile* (CD630_12870) and FurA from *Anabaena* sp. PCC 7120 (All1691) was

retrieved from KEGG Genes (https://www.genome.jp/kegg/genes.html). Pairwise sequence alignment of Fur proteins was carried out using UniProt ClustalO (https://www.expasy.org/resources/uniprot-clustalo). The corresponding UniProt IDs of *C. difficile* Fur and *Anabaena* sp. PCC 7120 FurA are Q18BE9 and Q7A2F4 and were obtained from (https://www.uniprot.org). PSIPRED server protein secondary structure prediction algorithm was used for secondary structure prediction (http://bioinf.cs.ucl.ac.uk/psipred/). Physicochemical properties of the proteins were deduced using the PROTPARAM tool (http://web.expasy.org/protparam) from ExPaSy Bioinformatics Resource Portal.

Acknowledgements

This work was funded by the Spanish Ministry of Economy, Industry and Competitiveness (BFU2016-77671-P) and the Government of Aragon-FEDER (B18, E35_23R), Institute of Health Carlos III (FIS: PI11/02578) and CIBERehd. ÁF-O was recipient of a PFIS fellowship from Institute of Health Carlos III (FI12/00482) and JG was recipient of a FPU fellowship from Ministry of Universities (FPU2018/03619). We thank Dr Rosa Bolea (Veterinary Faculty, Zaragoza University) for providing genomic DNA from *C. difficile* reference strain ATCC 43255 and Dr Klaus Hantke (IMIT, Tübingen University) for generously providing *E. coli* strain H1780. We also thank Dr Luc Ponchon (University París Descartes) for the gift of plasmid pACYCT2. We appreciate Dr Isabelle Michaud-Soret (CEA, Grenoble), Dr Andrés González (Department of Biochemistry and Molecular and Cellular Biology, Faculty of Sciences, University of Zaragoza) and Dr Jesús Arenas (Unit of Microbiology and Immunology, Faculty of Veterinary, University of Zaragoza) for critical discussion of results. Authors thank Dr Mónica Balsera (Instituto de Recursos Naturales y Agrobiología, CSIC) for recombinant *Ec*NTR and *Ec*Trx1.

Conflict of interest

The authors declare no conflict of interest.

Author contributions

ÁF-O, JG and MTB planned experiments. ÁF-O, JG and CS-B performed experiments. ÁF-O, JG, CS-B, MLP, MFF, ÁL and MTB analyzed data. ÁL and MFF contributed reagents or other essential material. JG and MTB wrote the paper.

Data availability statement

The data supporting the findings of this study are included in the main section of the manuscript. Further inquiries can be directed to the corresponding author.

References

1 Lawson PA, Citron DM, Tyrrell KL & Finegold SM (2016) Reclassification of *Clostridium difficile* as *Clostridioides difficile* (hall and O'Toole 1935) Prevot 1938. *Anaerobe* **40**, 95–99.
2 Mylonakis E, Ryan ET & Calderwood SB (2001) *Clostridium difficile*–associated diarrhea: a review. *Arch Intern Med* **161**, 525–533.
3 Kuijper EJ, Coignard B & Tull P (2006) Emergence of *Clostridium difficile*-associated disease in North America and Europe. *Clin Microbiol Infect* **12**(Suppl 6), 2–18.
4 Abdullatif VN & Noymer A (2016) *Clostridium difficile* infection: an emerging cause of death in the twenty-first century. *Biodemography Soc Biol* **62**, 198–207.
5 Peng Z, Jin D, Kim HB, Stratton CW, Wu B, Tang YW & Sun X (2017) Update on antimicrobial resistance in *Clostridium difficile*: resistance mechanisms and antimicrobial susceptibility testing. *J Clin Microbiol* **55**, 1998–2008.
6 Chong PM, Lynch T, McCorrister S, Kibsey P, Miller M, Gravel D, Westmacott GR, Mulvey MR & Canadian Nosocomial Infection Surveillance, P (2014) Proteomic analysis of a NAP1 *Clostridium difficile* clinical isolate resistant to metronidazole. *PLoS One* **9**, e82622.
7 Moura I, Monot M, Tani C, Spigaglia P, Barbanti F, Norais N, Dupuy B, Bouza E & Mastrantonio P (2014) Multidisciplinary analysis of a nontoxigenic *Clostridium difficile* strain with stable resistance to metronidazole. *Antimicrob Agents Chemother* **58**, 4957–4960.
8 Janoir C, Deneve C, Bouttier S, Barbut F, Hoys S, Caleechum L, Chapeton-Montes D, Pereira FC, Henriques AO, Collignon A *et al.* (2013) Adaptive strategies and pathogenesis of *Clostridium difficile* from in vivo transcriptomics. *Infect Immun* **81**, 3757–3769.
9 Deshpande A, Olaitan AO, McKelvey AM, Rutherford JT & Hurdle JG (2022) The ferrous iron transporter FeoB1 is essential for *Clostridioides difficile* toxin production and pathogenesis in mice. *bioRxiv* 10.1101/2022.03.03.482942 [PREPRINT]
10 Hastie JL, Hanna PC & Carlson PE (2018) Transcriptional response of *Clostridium difficile* to low iron conditions. *Pathog Dis* **76**, fty009.
11 Troxell B & Hassan HM (2013) Transcriptional regulation by ferric uptake regulator (fur) in pathogenic bacteria. *Front Cell Infect Microbiol* **3**, 59.

12 Hantke K (2001) Iron and metal regulation in bacteria. *Curr Opin Microbiol* **4**, 172–177.
13 Seo SW, Kim D, Latif H, O'Brien EJ, Szubin R & Palsson BO (2014) Deciphering fur transcriptional regulatory network highlights its complex role beyond iron metabolism in *Escherichia coli*. *Nat Commun* **5**, 4910.
14 Porcheron G & Dozois CM (2015) Interplay between iron homeostasis and virulence: fur and RyhB as major regulators of bacterial pathogenicity. *Vet Microbiol* **179**, 2–14.
15 Butler CA, Dashper SG, Zhang L, Seers CA, Mitchell HL, Catmull DV, Glew MD, Heath JE, Tan Y, Khan HS *et al*. (2014) The *Porphyromonas gingivalis* ferric uptake regulator orthologue binds hemin and regulates hemin-responsive biofilm development. *PLoS One* **9**, e111168.
16 González A, Bes MT, Barja F, Peleato ML & Fillat MF (2010) Overexpression of FurA in *Anabaena* sp. PCC 7120 reveals new targets for this regulator involved in photosynthesis, iron uptake and cellular morphology. *Plant Cell Physiol* **51**, 1900–1914.
17 González A, Angarica VE, Sancho J & Fillat MF (2014) The FurA regulon in *anabaena* sp. PCC 7120: in silico prediction and experimental validation of novel target genes. *Nucleic Acids Res* **42**, 4833–4846.
18 González A, Bes MT, Peleato ML & Fillat MF (2016) Expanding the role of FurA as essential global regulator in cyanobacteria. *PLoS One* **11**, e0151384.
19 Escolar L, Pérez-Martín J & de Lorenzo V (1999) Opening the iron box: transcriptional metalloregulation by the fur protein. *J Bacteriol* **181**, 6223–6229.
20 Winterbourn CC (1995) Toxicity of iron and hydrogen peroxide: the Fenton reaction. *Toxicol Lett* **82–83**, 969–974.
21 Bereswill S, Greiner S, van Vliet AH, Waidner B, Fassbinder F, Schiltz E, Kusters JG & Kist M (2000) Regulation of ferritin-mediated cytoplasmic iron storage by the ferric uptake regulator homolog (fur) of *Helicobacter pylori*. *J Bacteriol* **182**, 5948–5953.
22 Katigbak J & Zhang Y (2012) Iron binding site in a global regulator in bacteria - ferric uptake regulator (fur) protein: structure, Mossbauer properties, and functional implication. *J Phys Chem Lett* **2012**, 3503–3508.
23 Fillat MF (2014) The FUR (ferric uptake regulator) superfamily: diversity and versatility of key transcriptional regulators. *Arch Biochem Biophys* **546**, 41–52.
24 Dian C, Vitale S, Leonard GA, Bahlawane C, Fauquant C, Leduc D, Muller C, de Reuse H, Michaud-Soret I & Terradot L (2011) The structure of the *Helicobacter pylori* ferric uptake regulator fur reveals three functional metal binding sites. *Mol Microbiol* **79**, 1260–1275.
25 Butcher J, Sarvan S, Brunzelle JS, Couture JF & Stintzi A (2012) Structure and regulon of *Campylobacter jejuni* ferric uptake regulator fur define apo-fur regulation. *Proc Natl Acad Sci USA* **109**, 10047–10052.
26 Botello-Morte L, Pellicer S, Sein-Echaluce VC, Contreras LM, Neira JL, Abián O, Velázquez-Campoy A, Peleato ML, Fillat MF & Bes MT (2016) Cysteine mutational studies provide insight into a thiol-based redox switch mechanism of metal and DNA binding in FurA from *Anabaena* sp. PCC 7120. *Antioxid Redox Signal* **24**, 173–185.
27 Ho TD & Ellermeier CD (2015) Ferric uptake regulator fur control of putative iron acquisition systems in *Clostridium difficile*. *J Bacteriol* **197**, 2930–2940.
28 Berges M, Michel AM, Lassek C, Nuss AM, Beckstette M, Dersch P, Riedel K, Sievers S, Becher D, Otto A *et al*. (2018) Iron regulation in *Clostridioides difficile*. *Front Microbiol* **9**, 3183.
29 Weiss A, López CA, Beavers WN, Rodríguez J & Skaar EP (2021) *Clostridioides difficile* strain-dependent and strain-independent adaptations to a microaerobic environment. *Microb Genom* **7**, 000738.
30 Lynch T, Chong P, Zhang J, Hizon R, Du T, Graham MR, Beniac DR, Booth TF, Kibsey P, Miller M *et al*. (2013) Characterization of a stable, metronidazole-resistant *Clostridium difficile* clinical isolate. *PLoS One* **8**, e53757.
31 Monaghan TM, Chilton CH, Fit M, Buckley AM, Kuehne SA, Wilcox MH & Cockayne A (2016) Mutation of the ferric uptake regulator (fur) severely impairs toxin production in a human in vitro gut model of *Clostridium difficile* infection. *Gut* **65**, A25–A26.
32 Heidrich C, Hantke K, Bierbaum G & Sahl HG (1996) Identification and analysis of a gene encoding a fur-like protein of *Staphylococcus epidermidis*. *FEMS Microbiol Lett* **140**, 253–259.
33 Hantke K (1987) Selection procedure for deregulated iron transport mutants (fur) in *Escherichia coli* K 12: fur not only affects iron metabolism. *Mol Gen Genet* **210**, 135–139.
34 Pellicer S, Bes MT, González A, Neira JL, Peleato ML & Fillat MF (2010) High-recovery one-step purification of the DNA-binding protein fur by mild guanidinium chloride treatment. *Process Biochem* **45**, 292–296.
35 Pellicer S, González A, Peleato ML, Martínez JI, Fillat MF & Bes MT (2012) Site-directed mutagenesis and spectral studies suggest a putative role of FurA from *Anabaena* sp. PCC 7120 as a heme sensor protein. *FEBS J* **279**, 2231–2246.
36 Hernández JA, Bes MT, Fillat MF, Neira JL & Peleato ML (2002) Biochemical analysis of the recombinant fur (ferric uptake regulator) protein from *Anabaena* PCC 7119: factors affecting its oligomerization state. *Biochem J* **366**, 315–322.

37 Jones DT (1999) Protein secondary structure prediction based on position-specific scoring matrices. *J Mol Biol* **292**, 195–202.

38 Pohl E, Haller JC, Mijovilovich A, Meyer-Klaucke W, Garman E & Vasil ML (2003) Architecture of a protein central to iron homeostasis: crystal structure and spectroscopic analysis of the ferric uptake regulator. *Mol Microbiol* **47**, 903–915.

39 Deng Z, Wang Q, Liu Z, Zhang M, Machado AC, Chiu TP, Feng C, Zhang Q, Yu L, Qi L *et al.* (2015) Mechanistic insights into metal ion activation and operator recognition by the ferric uptake regulator. *Nat Commun* **6**, 7642.

40 Girinathan BP, Braun SE & Govind R (2014) *Clostridium difficile* glutamate dehydrogenase is a secreted enzyme that confers resistance to H_2O_2. *Microbiology* **160**, 47–55.

41 Hunt JB, Neece SH & Ginsburg A (1985) The use of 4-(2-pyridylazo)resorcinol in studies of zinc release from *Escherichia coli* aspartate transcarbamoylase. *Anal Biochem* **146**, 150–157.

42 Banci L, Bertini I, Boca M, Girotto S, Martinelli M, Valentine JS & Vieru M (2008) SOD1 and amyotrophic lateral sclerosis: mutations and oligomerization. *PLoS One* **3**, e1677.

43 Laitaoja M, Valjakka J & Janis J (2013) Zinc coordination spheres in protein structures. *Inorg Chem* **52**, 10983–10991.

44 Vitale S, Fauquant C, Lascoux D, Schauer K, Saint-Pierre C & Michaud-Soret I (2009) A ZnS(4) structural zinc site in the *Helicobacter pylori* ferric uptake regulator. *Biochemistry* **48**, 5582–5591.

45 Delany I, Spohn G, Rappuoli R & Scarlato V (2003) An anti-repression fur operator upstream of the promoter is required for iron-mediated transcriptional autoregulation in *Helicobacter pylori*. *Mol Microbiol* **50**, 1329–1338.

46 Ledala N, Pearson SL, Wilkinson BJ & Jayaswal RK (2007) Molecular characterization of the fur protein of *Listeria monocytogenes*. *Microbiology (Reading)* **153**, 1103–1111.

47 Sestok AE, Linkous RO & Smith AT (2018) Toward a mechanistic understanding of Feo-mediated ferrous iron uptake. *Metallomics* **10**, 887–898.

48 Sandmann G & Malkin R (1983) Iron-sulfur centers and activities of the photosynthetic electron transport chain in iron-deficient cultures of the blue-green alga aphanocapsa. *Plant Physiol* **73**, 724–728.

49 de Lorenzo V, Wee S, Herrero M & Neilands JB (1987) Operator sequences of the aerobactin operon of plasmid ColV-K30 binding the ferric uptake regulation (*fur*) repressor. *J Bacteriol* **169**, 2624–2630.

50 Meyer Y, Buchanan BB, Vignols F & Reichheld JP (2009) Thioredoxins and glutaredoxins: unifying elements in redox biology. *Annu Rev Genet* **43**, 335–367.

51 Guío J, Bes MT, Balsera M, Calvo-Begueria L, Sevilla E, Peleato ML & Fillat MF (2021) Thioredoxin dependent changes in the redox states of FurA from *anabaena* sp. PCC 7120. *Antioxidants* **10**, 913.

52 Buey RM, Galindo-Trigo S, López-Maury L, Velázquez-Campoy A, Revuelta JL, Florencio FJ, de Pereda JM, Schürmann P, Buchanan BB & Balsera M (2017) A new member of the thioredoxin reductase family from early oxygenic photosynthetic organisms. *Mol Plant* **10**, 212–215.

53 Hajjaji HE, Dumoulin M, Matagne A, Colau D, Roos G, Messens J & Collet J-F (2009) The zinc center influences the redox and thermodynamic properties of *Escherichia coli* thioredoxin 2. *J Mol Biol* **386**, 60–71.

54 Bhattacharyya A, Chattopadhyay R, Mitra S & Crowe SE (2014) Oxidative stress: an essential factor in the pathogenesis of gastrointestinal mucosal diseases. *Physiol Rev* **94**, 329–354.

55 Fang FC, Frawley ER, Tapscott T & Vazquez-Torres A (2016) Bacterial stress responses during host infection. *Cell Host Microbe* **20**, 133–143.

56 Quatrini R, Lefimil C, Holmes DS & Jedlicki E (2005) The ferric iron uptake regulator (fur) from the extreme acidophile *Acidithiobacillus ferrooxidans*. *Microbiology (Reading)* **151**, 2005–2015.

57 Ernst FD, Homuth G, Stoof J, Mader U, Waidner B, Kuipers EJ, Kist M, Kusters JG, Bereswill S & van Vliet AH (2005) Iron-responsive regulation of the *Helicobacter pylori* iron-cofactored superoxide dismutase SodB is mediated by fur. *J Bacteriol* **187**, 3687–3692.

58 Carpenter BM, Gilbreath JJ, Pich OQ, McKelvey AM, Maynard EL, Li ZZ & Merrell DS (2013) Identification and characterization of novel *Helicobacter pylori* apo-fur-regulated target genes. *J Bacteriol* **195**, 5526–5539.

59 Ernst FD, Bereswill S, Waidner B, Stoof J, Mäder U, Kusters JG, Kuipers EJ, Kist M, van Vliet AHM & Homuth G (2005) Transcriptional profiling of *Helicobacter pylori* fur- and iron-regulated gene expression. *Microbiology* **151**, 533–546.

60 Gancz H, Censini S & Merrell DS (2006) Iron and pH homeostasis intersect at the level of fur regulation in the gastric pathogen *Helicobacter pylori*. *Infect Immun* **74**, 602–614.

61 Latifi A, Jeanjean R, Lemeille S, Havaux M & Zhang C-C (2005) Iron starvation leads to oxidative stress in *Anabaena* sp. strain PCC 7120. *J Bacteriol* **187**, 6596–6598.

62 Leaden L, Silva LG, Ribeiro RA, dos Santos NM, Lorenzetti APR, Alegria TGP, Schulz ML, Medeiros MHG, Koide T & Marques MV (2018) Iron deficiency generates oxidative stress and activation of the SOS response in *Caulobacter crescentus*. *Front Microbiol* **9**, 2014.

63 Neumann-Schaal M, Metzendorf NG, Troitzsch D, Nuss AM, Hofmann JD, Beckstette M, Dersch P, Otto A & Sievers S (2018) Tracking gene expression and oxidative damage of O_2-stressed *Clostridioides difficile* by a multi-omics approach. *Anaerobe* **53**, 94–107.
64 Althaus EW, Outten CE, Olson KE, Cao H & O'Halloran TV (1999) The ferric uptake regulation (fur) repressor is a zinc metalloprotein. *Biochemistry* **38**, 6559–6569.
65 Lill R (2020) Do FeS clusters rule bacterial iron regulation? *J Biol Chem* **295**, 15464–15465.
66 Fontenot CR, Tasnim H, Valdes KA, Popescu CV & Ding H (2020) Ferric uptake regulator (fur) reversibly binds a [2Fe-2S] cluster to sense intracellular iron homeostasis in *Escherichia coli*. *J Biol Chem* **295**, 15454–15463.
67 Fontenot CR & Ding H (2022) Ferric uptake regulators (fur) from *Vibrio cholerae* and *Helicobacter pylori* bind a [2Fe-2S] cluster in response to elevation of intracellular free iron content. *Biometals* **35**, 591–600.
68 Nesbit AD, Giel JL, Rose JC & Kiley PJ (2009) Sequence-specific binding to a subset of IscR-regulated promoters does not require IscR Fe-S cluster ligation. *J Mol Biol* **387**, 28–41.
69 Ellman GL (1959) Tissue sulfhydryl groups. *Arch Biochem Biophys* **82**, 70–77.

Supporting information

Additional supporting information may be found online in the Supporting Information section at the end of the article.

Table S1. Bacterial strains and plasmids used in this study.

Table S2. PCR primers used in this study.